Cancer Science
The official journal of the Japanese Cancer Association JCA

Dofequidar fumarate sensitizes cancer stem-like side population cells to chemotherapeutic drugs by inhibiting ABCG2/BCRP-mediated drug export

Ryohei Katayama,[1] Sumie Koike,[1] Shigeo Sato,[1] Yoshikazu Sugimoto,[1,2] Takashi Tsuruo[1] and Naoya Fujita[1,3]

[1]Cancer Chemotherapy Center, Japanese Foundation for Cancer Research; [2]Graduate School of Pharmaceutical Sciences, Keio University, Tokyo, Japan

(Received June 15, 2009/Revised July 07, 2009/Accepted July 08, 2009/Online publication August 9, 2009)

The ATP-binding cassette (ABC) transporters (ABC-T) actively efflux structurally and mechanistically unrelated anticancer drugs from cells. As a consequence, they can confer multidrug resistance (MDR) to cancer cells. ABC-T are also reported to be phenotypic markers and functional regulators of cancer stem/initiating cells (CSC) and believed to be associated with tumor initiation, progression, and relapse. Dofequidar fumarate, an orally active quinoline compound, has been reported to overcome MDR by inhibiting ABCB1/P-gp, ABCC1/MDR-associated protein 1, or both. Phase III clinical trials suggested that dofequidar had efficacy in patients who had not received prior therapy. Here we show that dofequidar inhibits the efflux of chemotherapeutic drugs and increases the sensitivity to anticancer drugs in CSC-like side population (SP) cells isolated from various cancer cell lines. Dofequidar treatment greatly reduced the cell number in the SP fraction. Estimation of ABC-T expression revealed that ABCG2/breast cancer resistance protein (BCRP) mRNA level, but not the ABCB1/P-gp or ABCC1/MDR-associated protein 1 mRNA level, in all the tested SP cells was higher than that in non-SP cells. The *in vitro* vesicle transporter assay clarified that dofequidar had the ability to suppress ABCG2/BCRP function. Dofequidar treatment sensitized SP cells to anticancer agents *in vitro*. We compared the antitumor efficacy of irinotecan (CPT-11) alone with that of CPT-11 plus dofequidar in xenografted SP cells. Although xenografted SP tumors showed resistance to CPT-11, treatment with CPT-11 plus dofequidar greatly reduced the SP-derived tumor growth *in vivo*. Our results suggest the possibility of selective eradication of CSC by inhibiting ABCG2/BCRP. (*Cancer Sci* 2009; 100: 2060–2068)

Although conventional chemotherapy kills most tumor cells, it is believed to leave some cells behind, which might be the source of recurrence. The cells that tend to remain are thought to be cancer stem cells (CSC).[1] CSC are likely to share many properties of normal stem cells, such as a resistance to drugs and toxins through the expression of several ATP-binding cassette (ABC) transporters (ABC-T). Therefore, tumors might have a built-in population of drug-resistant pluripotent cells that can survive after chemotherapy and can repopulate the tumor.

The drug-transporting properties of some ABC-T are important markers for isolation and analysis of stem cells. Most differentiated cells accumulate the fluorescent dye Hoechst33342, but stem cells cannot accumulate the dye because of its active efflux via ABC-T. Thus, stem cells can be concentrated by collecting a population that contains only a low level of Hoechst33342 fluorescence.[2,3] These cells are referred to as side population (SP) cells. A large fraction of hematopoietic stem cells are found in the SP fraction.[4] SP cells can be isolated from many normal tissues,[3,5,6] which were enriched in lineage-specific stem cell. SP cells can be also identified in some neuroblastoma, hepatocellular carcinoma, gastrointestinal cancer, and glioblastoma cells, and in several cell lines that have been maintained in culture over long periods of time.[7–10]

By inhibiting the major transporters, tumor elimination could be achieved by reversing drug resistance. Therefore, many efforts have been devoted to developing inhibitors against ABC-T. Since the discovery of verapamil as a multidrug resistance (MDR)-reversing agent,[11] many compounds have been investigated as MDR inhibitors.[12] Most of the compounds, however, do not exhibit positive results in animal studies because of their dose-limiting toxicity.[12]

We previously reported a series of quinoline derivatives that show MDR-reversing activities in K562 cells that are resistant to doxorubicin (K562/ADM).[13] K562/ADM is a human leukemia cell line that endogenously overexpresses ABCB1/P-gp. Among these derivatives, dofequidar fumarate (dofequidar) was identified as a novel, orally active, quinoline-derivative inhibitor of ABCB1/P-gp. In preclinical studies, dofequidar reversed MDR in ABCB1/P-gp-expressing and ABCC1/MDR-associated protein (MRP) 1-expressing cancer cells *in vitro*. In addition, oral administration of dofequidar enhanced the antitumor activity of doxorubicin (ADM), vincristine, and docetaxel *in vivo*.[14–16] Thus, dofequidar is a promising MDR-reversing agent. The results of phase III clinical evaluations of dofequidar for breast cancer patients showed a relative improvement and absolute increase in response rate for patients who received dofequidar plus cyclophosphamide, doxorubicin, and fluorouracil (CAF), but the findings did not reach statistical significance. However, subgroup analysis suggested that dofequidar plus CAF therapy displayed significantly improved, progression-free survival and overall survival in patients who had not received prior therapy.[17]

Irinotecan (CPT-11) is one of the most widely prescribed drugs for many cancers.[18] It is reported that CPT-11 is exported from the cells by ABCB1/P-gp and ABCC1/MRP1.[19,20] In addition, SN-38, the active metabolite of prodrug CPT-11, is exported from the cells by ABCG2/breast cancer resistance protein (BCRP),[21] and the therapeutic efficacy of CPT-11 is strongly correlated with BCRP expression. Therefore, in the present study, we tried to evaluate the antitumor activity of dofequidar combined with CPT-11.

In the present study, we found that SP cells from various cancer cell lines exhibited MDR properties. Treatment of SP cells with dofequidar reversed the MDR phenotype by inhibiting ABCG2/BCRP. Dofequidar also reversed the drug resistance of xenografted SP cells *in vivo*. These results suggest that dofequidar may show clinical efficacy and may improve progression-free survival by inhibiting ABCG2/BCRP that is overexpressed specifically in CSC.

Material and Methods

Reagents and cell culture conditions. Fumitremorgin C (FTC) and reserpine were purchased from Alexis Corp. (Lausen,

[3]To whom correspondence should be addressed. E-mail: naoya.fujita@jfcr.or.jp

doi: 10.1111/j.1349-7006.2009.01288.x

Switzerland) and Daiichi Pharmaceutical (Tokyo, Japan), respectively. Mitoxantrone (MXR) and methotrexate (MTX) were purchased from Sigma (St. Louis, MO, USA) and Biomol International L.P. (Exeter, UK), respectively. Dofequidar and CPT-11 were kindly provided by Bayer Schering Pharma (Osaka, Japan) and Yakult Honsha Co. (Tokyo, Japan), respectively. Human cervix carcinoma HeLa cells, human epidermoid carcinoma KB-3-1 cells, and the stable transfectants of KB-3-1 cells were cultured in DMEM supplemented with 10% FBS (DMEM growth medium). Human chronic myeloid leukemia K562 and the stable transfectants, human breast cancer BSY-1, HBC-4, and HBC-5, human glioma U251, human pancreatic cancer Capan-1, human colon cancer KM12, and human stomach cancer MKN74 were cultured in RPMI-1640 medium supplemented with 10% FBS. To assess the cell viability, cells were incubated with 3-(4,5-dimethylthiazol-2-yl)-5-(3-carboxymethoxyphenyl)-2-(4-sulfophenyl)-2H-tetrazolium (MTS) (Promega, Madison, WI, USA) for 1 h and the optical density was measured using a microplate spectrophotometer (Benchmark-Plus; Bio-Rad, Richmond, CA, USA).

Analysis and SP cell sorting from various cancer cell lines using FACS Vantage. Cells were trypsinized and resuspended in ice-cold HBSS supplemented with 2% FBS at a concentration of 1×10^6 cells/mL. For SP analysis, cells were treated with 2.5–15 μg/mL Hoechst33342 dye (Invitrogen, Carlsbad, CA, USA) for 60 min at 37°C with or without ABC-T inhibitors (reserpine, FTC, or dofequidar). After washing with PBS, 3×10^4 cells were analyzed using a FACS Vantage SE flow cytometer (BD Bioscience, San Jose, CA, USA). Analysis was done using Flow Jo software (Treestar, San Carlos, CA, USA).

RNA preparation and real-time PCR. Total RNA from HeLa SP and non-SP (NSP) cells were extracted using an RNeasy Mini Kit (Qiagen, Hiden, Germany). RNA (1 μg) was reverse transcribed using SuperScript III (Invitrogen), according to the manufacturer's instructions. Then, the amount of ABCG2, ABCB1, and ABCC1 mRNA was quantified with TaqMan probes using a PCR LightCycler 480 (Roche Diagnostics, Basel, Switzerland) and normalized to the amount of GAPDH mRNA. The sequences of the primers for ABC-T are described in Table S1.

***In vivo* tumorigenicity and treatment.** Sorted HeLa SP and NSP cells were collected and resuspended in DMEM growth medium at concentrations ranging from 100 to 10 000 cells/30 μL. Cells were then mixed with 30 μL of Matrigel (BD Bioscience). This cell–Matrigel suspension was injected s.c. into 5- to 6-week-old female BALB/c-*nu/nu* (nude) mice (Charles River Laboratories, Yokohama, Japan). The mice were checked twice weekly for palpable tumor formation. The mice were then euthanized and tumors were resected and diced. A piece of tumor was sequentially injected s.c. into another 5- to 6-week-old female BALB/c nude mouse. Tumor size was measured every second day with a caliper, and tumor volumes were defined as (longest diameter) × (shortest diameter)/2.[2] When tumor size was approximately 100 mm^3, mice were sorted into four equal groups. Then, the nude mice were administered orally with dofequidar (200 mg/kg) or water as a control, 30 min before intravenous administration of CPT-11 (67 mg/kg) on days 0, 4, and 8. Bodyweight and tumor size were measured every 3 days. All animal procedures were carried out using protocols approved by the Japanese Foundation for Cancer Research Animal Care and Use Committee.

Transfection and immunoblotting. Negative control siRNA (medium GC duplex), ABCG2-1 siRNA, and ABCG2-2 siRNA were purchased from Invitrogen (Table S1). HeLa cells were transfected with various siRNA with LipofectAMINE 2000 reagent (Invitrogen), according to the manufacturer's instructions. After 24 h of incubation, cells were harvested, and the expression of ABCG2/BCRP and the cell number in the SP fraction was analyzed. For immunofluorescent staining, cells were incubated in blocking buffer (5 mg/mL of BSA and 2 mM EDTA in PBS) for 15 min. Then, 0.5 μg of biotin-conjugated anti-ABCG2/BCRP antibody (5D3; eBioscience, San Diego, CA, USA) was added. After incubation for 30 min, cells were washed and incubated with 0.1 μg of streptavidin–phycoerythrin (PE) (BD Bioscience). After washing, cells were analyzed by flow cytometry. For immunoblotting, cells were lysed in SDS sample buffer (0.1 M Tris-HCl at pH 8.0, 10% glycerol, and 1% SDS) with sonication and cleared by centrifugation at 17 400*g* for 10 min. Samples were electrophoresed and immunoblotted with the indicated antibodies: ABCG2/BCRP polyclonal antibody,[22] MDR1 antibody (JSB-1; Monosan, Uden, the Netherlands), MRP1 antibody (MRPm6, Monosan), and tubulin alpha antibody (YL1/2; Serotec, Oxford, UK).

***In vitro* vesicle transport assay.** We assayed ^{3}H-labeled MTX ([^{3}H]MTX) transport using lipid vesicles containing ABCG2/BCRP protein (Genomembrane, Yokohama, Japan), according to the manufacturer's instructions. [^{3}H]MTX was purchased from Moravek (Brea, CA, USA) (#MT701). The transport reaction (50 mM MOPS-Tris [pH 7.0], 7.5 mM $MgCl_2$, 70 mM KCl, 160 μM cold MTX, with various inhibitors [dofequidar, FTC, or verapamil], 1 mCi/mL [^{3}H]MTX, and membrane vesicles [25 μg protein]) in a 30-μL mixture was kept on ice for 5 min. Then, 20 μL of 10 mM ATP or AMP was added into reaction mixtures and incubated at 37°C for 5 min. The reaction was terminated by adding an ice-cold stop solution (40 mM MOPS-Tris [pH 7.0] and 70 mM KCl). The membrane vesicles were trapped on a TOPCOUNT plate filter and washed with ice-cold stop solution. The radioactivity was measured with a liquid scintillation counter (Topcount; Perkin Elmer, Waltham, MA, USA).

Intracellular drug accumulation. The effect of dofequidar on the intracellular accumulation of MXR was determined by flow cytometry. K562 or K562/BCRP cells (5×10^5 cells) were incubated with 3 μM MXR for 30 min at 37°C with or without dofequidar or FTC, washed in ice-cold PBS, and then subjected to fluorescence analysis using a Cytomics FC500 (Beckman Coulter, Fullerton, CA, USA) with 630 nm excitation.

Statistical analysis. All data are shown as means ± SD. Student's *t*-test was carried out. *P*-values <0.05 were considered statistically significant. All statistical tests were two sided.

Results

Identification and characterization of SP cells. Staining the cells with Hoechst33342 dye followed by flow cytometric analysis revealed the presence of a very small unstained population (i.e. the SP) of cells in primary tumors and several cell lines. SP cells are known to show cancer stem cell-like properties, such as high tumorigenicity and repopulating ability. To study the characteristics of SP cells and to develop new strategies targeting cancer stem cells, we first investigated the presence of SP cells in established human cancer cell lines. Consistent with a previous report,[10] the human cervical cancer HeLa cell line contained SP cells at approximately 0.5–1% of the total (Fig. 1A, left panels). The number of cells in the SP fraction derived from HeLa and HBC-4 cells was drastically reduced by adding the ABC-T inhibitor reserpine (Fig. 1A, right panels). Because reserpine treatment did not affect the fluorescence patterns of Hoechst33342-stained U251 glioma cells, we concluded that U251 glioma cells did not contain SP cells. However, the cell lines that contain no SP cells, like U251, might have CSC that don't overexpress ABC-T associated with Hoechst33342 efflux. We further examined the presence of SP cells in various cancer cell lines, and as shown in Figure 1(B), most cancer cell lines contained SP cells, whereas the SP fractions varied from 0.2 to 10%.

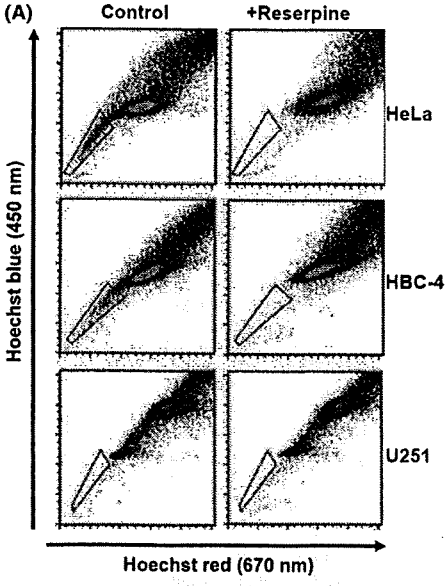

(B)

Cell lines	Tissue	SP
HeLa	Cervix	+
HBC-4	Breast	+
BSY-1	Breast	+
HBC-5	Breast	+
U251	Glioma (brain)	–
Capan-1	Pancreas	+
KM12	Colon	+
MKN74	Stomach	+

Fig. 1. The presence of side population (SP) cells in various cancer cell lines. (A) Cells were stained with Hoechst33342 in the presence (+reserpine) or absence (control) of reserpine, and were analyzed using FACS Vantage. The trapezia in each panel indicate the SP area. (B) Summary of the presence of SP cells in various human cancer cell lines. Cells were stained and the presence of SP cells examined, as described in (A). +, Presence of SP cells; –, absence of SP cells.

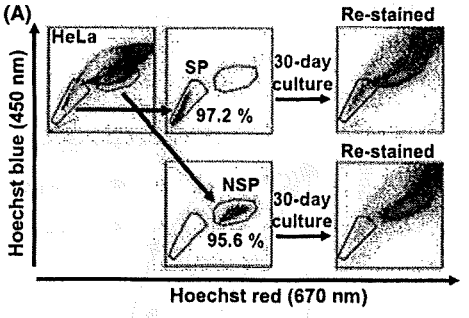

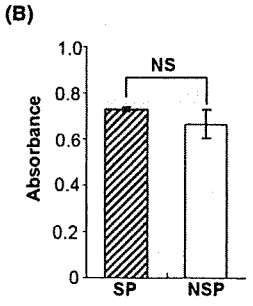

(C)

Tumor formation (HeLa, 60 days)				
Injected cell number	10^2	10^3	3×10^3	10^4
SP	6/6	6/6	6/6	5/5
NSP	6/6	6/6	6/6	6/6

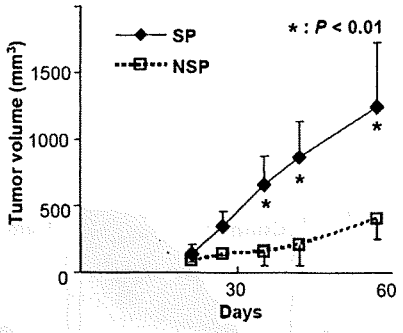

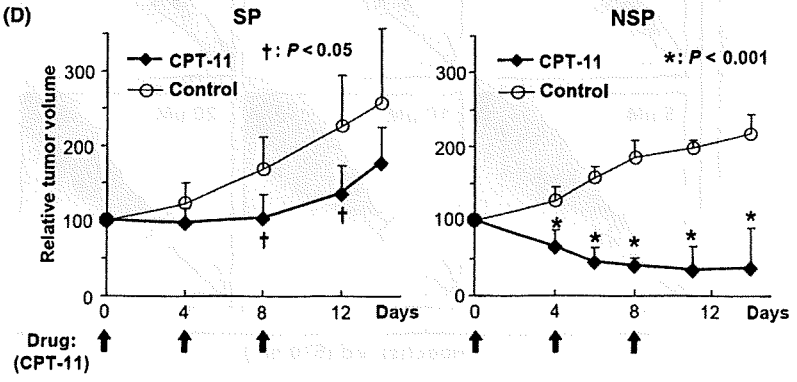

Fig. 2. Characteristics of side population (SP) cells. (A) SP and non-SP (NSP) fractions were sorted from HeLa cells. The sorting purities were confirmed by immediate reanalysis. After 30-day *in vitro* culture of the separated cells, cells were restained and analyzed (re-stained). (B) Two thousand sorted HeLa SP and NSP cells were incubated for 72 h, and the viable cell number was assessed by 3-(4,5-dimethylthiazol-2-yl)-5-(3-carboxymethoxyphenyl)-2-(4-sulfophenyl)-2H-tetrazolium (MTS) assay. No significant difference was observed between SP and NSP (NS, $P = 0.21$). (C) The indicated numbers of sorted HeLa SP and NSP cells were s.c. injected into BALB/c nude mice ($n = 6$ or 5). Tumor formation was assessed after 60 days (left). The growth of xenografts derived from one hundred sorted HeLa SP and NSP cells ($n = 6$, $^*P < 0.01$) (right). (D) The xenografted HeLa-derived SP and NSP tumors were cut into 2-mm cubes and transplanted into other mice. When secondary tumors reached approximately 100 mm^3 in volume, CPT-11 was administrated intravenously at 67 mg/kg on days 0, 4, and 8 (arrows). The graphs show the relative tumor volume ($n = 6$). ($^\dagger P < 0.05$, $^*P < 0.001$).

doi: 10.1111/j.1349-7006.2009.01288.x

To examine the characteristics of SP cells, we sorted the SP and NSP cells from HeLa using a cell sorter. After sorting, SP and NSP cells were cultured in DMEM growth medium for 30 days. The cells were restained with Hoechst33342 and analyzed by flow cytometry. As shown in Figure 2(A), SP cells derived from HeLa cells showed repopulating capacity. Although NSP cells could proliferate *in vitro*, at approximately the same speed as the SP cells (Fig. 2B), the SP cell number after 30-day culture of NSP cells was smaller than that of post-culture SP cells. Thus, HeLa-derived NSP cells had weak repopulating capacity. We checked several cell lines and confirmed that the isolated SP cells could repopulate (data not shown).

We next tested the tumorigenic ability of the isolated SP cells when grafted into nude mice. When HeLa-derived SP and NSP cells were s.c. injected into nude mice, both fractions exhibited similar tumor-forming abilities (Fig. 2C, left). Interestingly, tumors derived from HeLa SP cells grew faster than those from NSP cells (Fig. 2C, right). These results suggest that HeLa SP cells, which have the ability of self-renewal and repopulation, form more aggressive tumors in nude mice than do HeLa NSP cells. To evaluate the chemoresistance of SP cells, we inoculated SP and NSP cells derived from HeLa cells. To equalize the tumor volume, the tumors that formed first were transplanted into other nude mice. The secondary tumors derived from HeLa SP cells also grew faster than those from NSP cells (data not shown). When the secondarily formed tumor volume reached 100 mm^3, the mice were treated with CPT-11. In HeLa SP-bearing mice, 4-day intervals (q4d) × 3 treatments of CPT-11 (67 mg/kg) alone arrested tumor growth without reducing the tumor volume. After termination of CPT-11 treatment, the remaining tumor started to regrow (Fig. 2D, left). However, treatment of HeLa NSP cells with q4d × 3 of 67 mg/kg of CPT-11 alone drastically reduced the tumor volume (Fig. 2D, right). These results suggest that SP-derived tumor cells had robust chemoresistance.

Dofequidar reduced the SP cell ratio. Several reports suggest that CSC show resistance to chemotherapy by expressing such ABC-T as ABCB1/P-gp and ABCG2/BCRP.[1] SP cells also have the a exporting ability of Hoechst33342, which is a substrate of ABC-T (Fig. 1). Expression of ABC-T might be associated with drug resistance in SP cells (Fig. 2D). Dofequidar (Fig. 3A) is a MDR-reversing agent currently under clinical evaluation in phase III trials.[17] Therefore, we tested the effects of dofequidar on cancer stem-like SP cells. As shown in Figure 3(B), dofequidar treatment reduced the HeLa cell number in the SP fraction dose dependently. We obtained similar results using BSY-1 and KM12 cells (Fig. 3C). These results indicate that dofequidar suppressed Hoechst33342 export by inhibiting transporters highly expressed on SP cell surfaces but not by reducing the number of SP cells themselves.

Involvement of ABCG2/BCRP, ABCB1/MDR1, and ABCC1/MRP1 in Hoechst33342 efflux. Because SP cells were separated according to the exporting activity of Hoechst33342 dye, we tried to identify the ABC-T responsible for Hoechst33342 efflux.

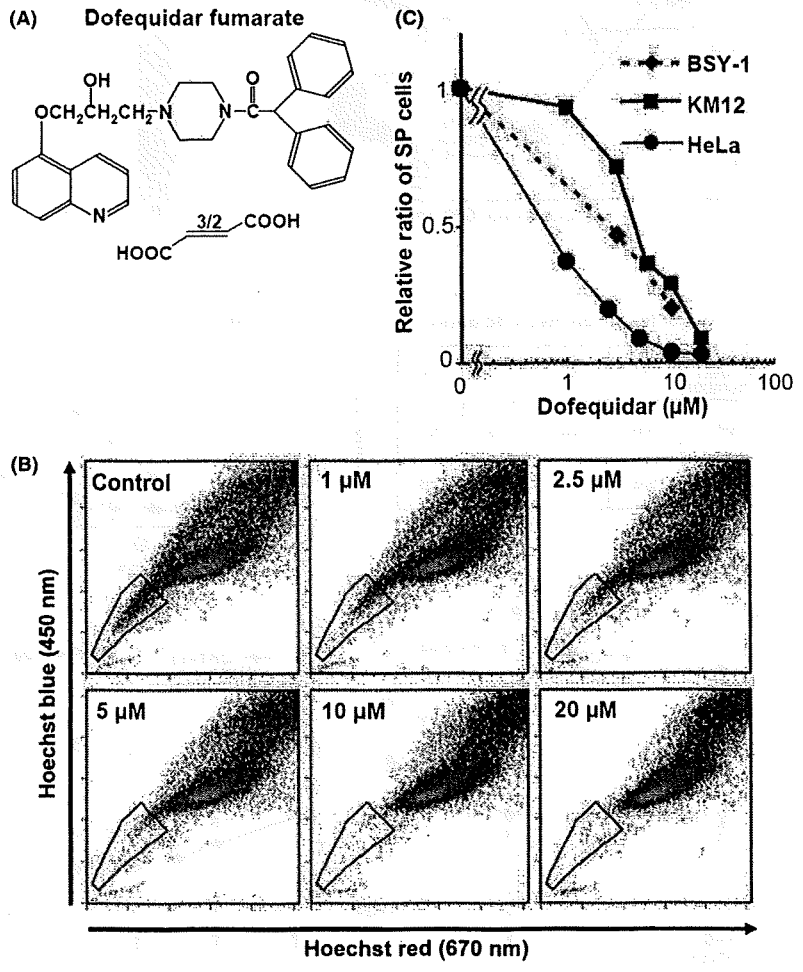

Fig. 3. Dofequidar reduced the cell number in the side population (SP) fraction. (A) Chemical structure of dofequidar. (B) HeLa cells were stained with 5 μg/mL Hoechst33342 in the presence of the indicated concentrations of dofequidar, and then analyzed. (C) Cells were stained and analyzed as in (B). The relative ratios of SP cell numbers in dofequidar-treated samples is shown by comparing with them with SP cell numbers in dofequidar-untreated samples.

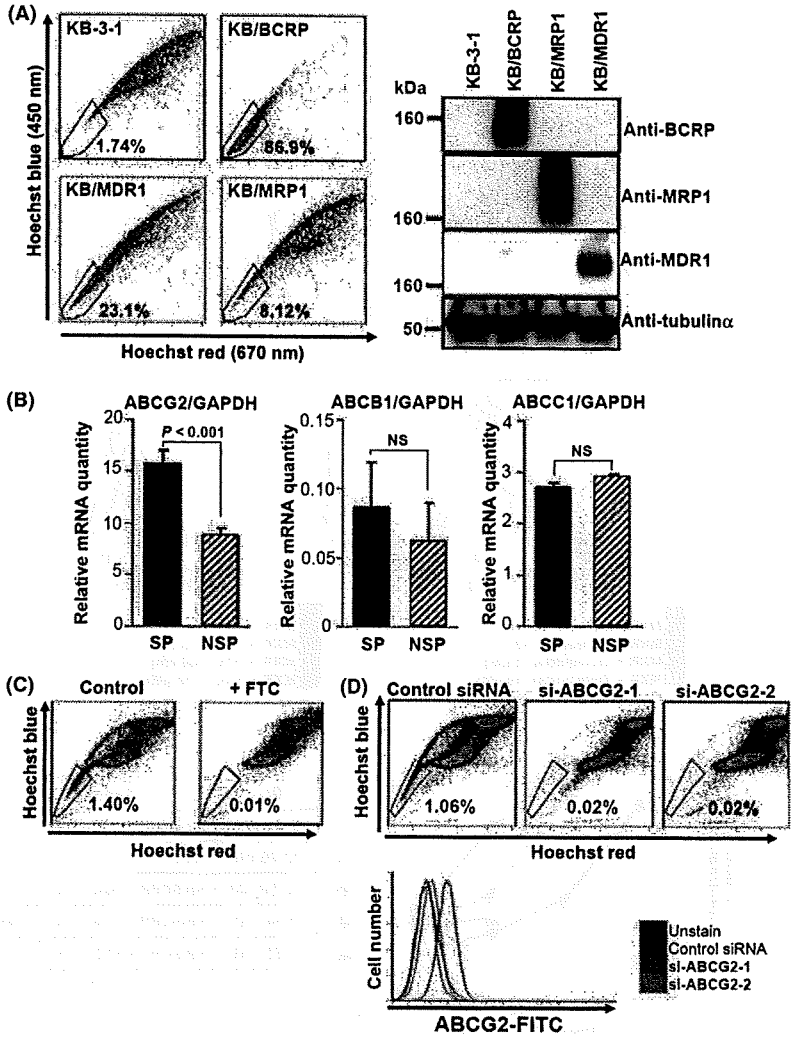

Fig. 4. Efflux of Hoechst33342 by ATP-binding cassette (ABC) G2/ABCG2/breast cancer resistance protein (BCRP), ABCB1/P-gp/multidrug resistance (MDR) 1, and ABCC1/MDR-associated protein (MRP) 1. (A) KB-3-1 and the stable transfectants were stained with Hoechst33342 and analyzed using FACS Vantage (left). The cell lysates from KB-3-1 and the stable transfectants were immunoblotted with the indicated antibodies (right). (B) mRNA was extracted from the sorted HeLa SP and NSP cells (solid and hatched columns, respectively). The graphs indicate relative mRNA expression levels of each ABC-transporter normalized with GAPDH. The expression level of ABCG2 mRNA in side population (SP) cells versus that in non-SP (NSP) cells was significantly different ($P < 0.001$). The expression levels of ABCB1 and ABCC1 mRNA were not significantly different (NS). (C) HeLa cells were stained with 5 μg/mL Hoechst33342 in the presence (+FTC) or absence (control) of 3 μM fumitremorgin C (FTC) and were analyzed. (D) HeLa cells were transfected with control siRNA or ABCG2 siRNA (si-ABCG2-1 and si-ABCG2-2). After transfection for 48 h, cells were stained with Hoechst33342 and analyzed (upper panels). The expression level of ABCG2/BCRP protein in the same samples were analyzed (lower panel).

Hoechst33342 was reported to be exported by several ABC-T, mainly ABCG2/BCRP; however, the targets of dofequidar were reported to be ABCB1/P-gp[13] and ABCC1/MRP1.[23] Then, we evaluated the Hoechst33342 export in ABCB1/P-gp-overexpressing KB-3-1 cells, ABCB1/P-gp-overexpressing KB-3-1 cells (KB/MDRI), ABCC1/MRP1-overexpressing KB-3-1 cells (KB/MRP1), and ABCG2/BCRP-overexpressing KB-3-1 cells (KB/BCRP)[22] As shown in Figure 4(A), overexpression of ABCB1/P-gp, ABCC1/MRP1, or ABCG2/BCRP in KB-3-1 cells increased the cell number in the SP fraction (23.1, 8.12, and 86.9%, respectively). Overexpression of each ABC-T did not affect the expression level of other ABC-T (Fig. 4A, right), suggesting that all of these ABC-T were associated with the Hoechst33342 efflux. We also observed that ABCG2/BCRP overexpression in K562 cells decreased Hoechst33342 blue (450 nm) fluorescence compared with parental K562 cells (Fig. S1A). We then compared the ABCB1, ABCC1, and ABCG2 mRNA expression in SP and NSP cells using a quantitative RT-PCR method. Unexpectedly, the expression levels of ABCB1 and ABCC1 mRNA were not significantly different between them. The ABCG2 mRNA expression in SP cells was significantly higher than that in NSP cells (Fig. 4B). We also observed elevated ABCG2/BCRP expression in SP cells derived from other cancer cells (data not shown). We examined the change in Hoechst33342 staining after FTC, a specific inhibitor of ABCG2/BCRP,[24] treatment, which resulted in a reduction of cell number in the SP fraction (Fig. 4C).

To further confirm the role of ABCG2/BCRP in Hoechst33342 dye efflux, we carried out Hoechst33342 staining after *ABCG2* gene silencing using two different ABCG2 siRNA. Both ABCG2 siRNA could almost completely downregulate the ABCG2/BCRP protein expression in HeLa cells (Fig. 4D, bottom panel). Under these conditions, we found a remarkable decrease in the SP cell number (Fig. 4D). These results strongly indicate that ABCG2/BCRP is mainly associated with the export of Hoechst33342 in HeLa SP cells.

Dofequidar inhibits ABCG2/BCRP in addition to ABCB1/P-gp and ABCC1/MRP1. Because dofequidar could reduce the cell number in the SP fraction that highly expressed ABCG2/BCRP (Figs 3,4), we hypothesized that dofequidar had the ability to inhibit ABCG2/BCRP in addition to the previously reported ABCB1/P-gp and ABCC1/MRP1.[13–16] Parental K562 cells or K562 stable transfectants were stained with Hoechst33342 in the presence or absence of ABC-T inhibitors. Dofequidar but not verapamil could increase the intracellular Hoechst33342 concentration in K562/BCRP cells dose dependently (Fig. S1B). We obtained similar results in KB/BCRP cells (data not shown).

doi: 10.1111/j.1349-7006.2009.01288.x

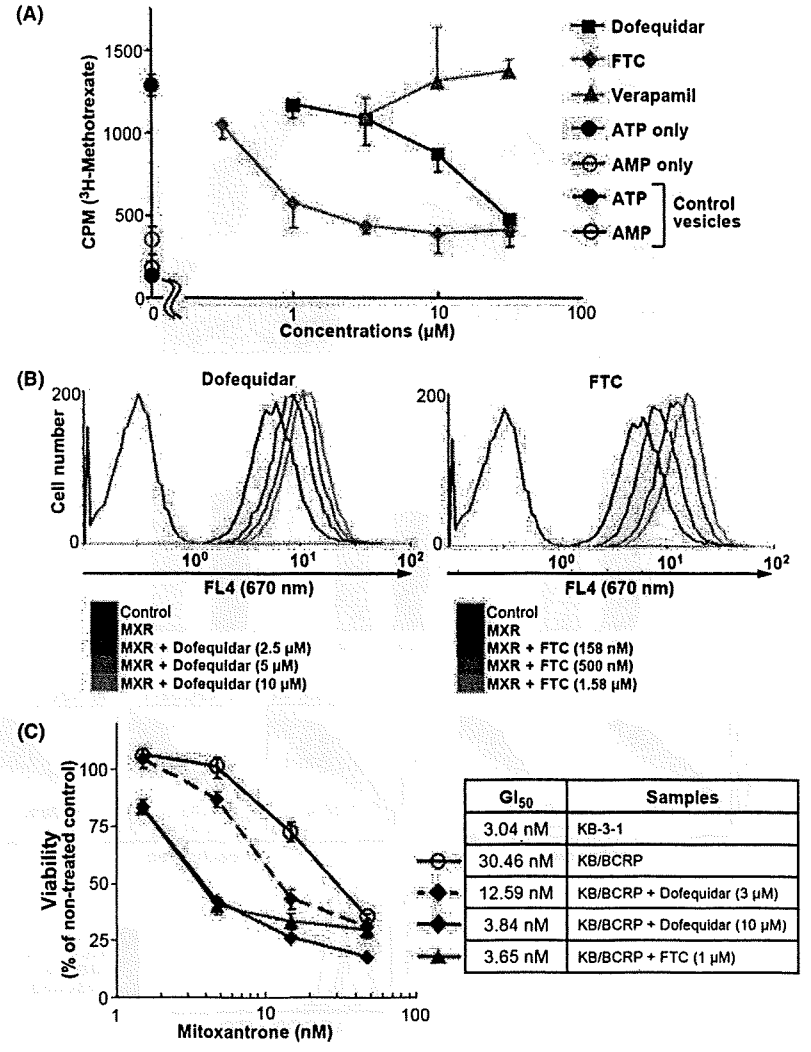

Fig. 5. Dofequidar inhibits ATP-binding cassette (ABC) G2/ABCG2/breast cancer resistantance protein (BCRP) *in vitro* and in cells. (A) Membrane vesicles from ABCG2/BCRP-overexpressing insect cells were incubated with ^{3}H-labeled methotrexate ([^{3}H]MTX) and ATP together with vehicle (ATP only) or the indicated concentrations of dofequidar, fumitremorgin C (FTC), or verapamil at 37°C. In some experiments, membrane vesicles were incubated with [^{3}H]MTX and AMP (AMP only). Membrane vesicles from control insect cells were also incubated with [^{3}H]MTX and ATP or AMP (control vesicles). After incubation for 5 min, the incorporated [^{3}H]MTX was assayed by liquid scintillation. (B) K562/BCRP cells were incubated with 3 μM mitoxantrone (MXR) together with vehicle or the indicated concentrations of dofequidar (MXR+Dofequidar, left panel) or FTC (MXR+FTC, right panel). In some experiments, K562/BCRP cells were incubated without drugs (control). After incubation for 30 min, the fluorescence of MXR at 670 nm was analyzed. (C) KB-3-1 and KB/BCRP cells were cultured in medium containing the indicated concentration of MXR with or without dofequidar or FTC for 3 days. Cell viability was evaluated using the 3-(4,5-dimethylthiazol-2-yl)-5-(3-carboxymethoxyphenyl)-2-(4-sulfophenyl)-2H-tetrazolium (MTS) method.

To confirm the result, we carried out an *in vitro* vesicle transport assay. Membrane vesicles from control or ABCG2/BCRP-overexpressing insect cells were incubated with [^{3}H]MTX in the presence of ATP or AMP. The ATP-dependent uptake of [^{3}H]MTX was observed in ABCG2/BCRP-overexpressing membrane vesicles but not in control vesicles (Fig. 4A). FTC and dofequidar, but not verapamil, inhibited [^{3}H]MTX uptake dose dependently (Fig. 5A). These results suggest that dofequidar had the ability to inhibit ABCG2/BCRP in addition to the previously reported ABCB1/P-gp and ABCC1/MRP1.[13–16]

ABCG2/BCRP is known to export various anticancer agents, such as MTX, MXR, topotecan, and SN-38, and cause chemoresistance.[25] Accordingly, we examined whether dofequidar could reverse chemoresistance by inhibiting ABCG2/BCRP function. First, we tested whether dofequidar inhibited the export of MXR in K562/BCRP cells. K562/BCRP cells were preincubated with dofequidar or FTC for 30 min, followed by MXR incubation in the presence of inhibitors. After 30 min of incubation, MXR incorporation was analyzed by flow cytometry. As a result dofequidar inhibited MXR export, like FTC (Fig. 5B). Second, we tested whether dofequidar induced cell death in KB/BCRP cells. KB/BCRP cells showed 10-fold resistance to MXR compared to parental KB-3-1 cells. Dofequidar could sensitize the KB/BCRP in a dose-dependent fashion. Treatment with 10 μM dofequidar reversed chemoresistance, to the same level as 1 μM FTC (Fig. 5C).

Dofequidar sensitized SP cells to anticancer agents. To overcome the chemoresistance of cancer stem-like SP cells, we examined the effects of dofequidar on chemosensitivity. Although HeLa-derived SP cells showed resistance to MXR and topotecan, compared with HeLa-derived NSP cells, adding dofequidar reversed the sensitivity to MXR and topotecan to a level similar to NSP cells (Fig. 6A). To confirm the results, SP and NSP cells were separated from breast cancer BSY-1 and HBC-5 cell lines and examined for changes in chemosensitivity after dofequidar treatment. SP cells derived from BSY-1 and HBC-5 cells showed two- to four-fold resistance to chemotherapy compared with NSP cells, and dofequidar effectively sensitized SP cells and decreased the 50% growth inhibition (GI_{50}) values to a level similar to NSP cells (Fig. 6A, lower table).

FTC is not suitable for clinical studies because of its severe toxicity, but it strongly and specifically inhibits ABCG2/BCRP.[26] On the other hand, dofequidar exhibits low toxicity and has already been approved for clinical trials. To overcome the chemoresistance of cancer stem-like SP cells *in vivo*, we evaluated the antitumor activity of CPT-11 plus dofequidar in a

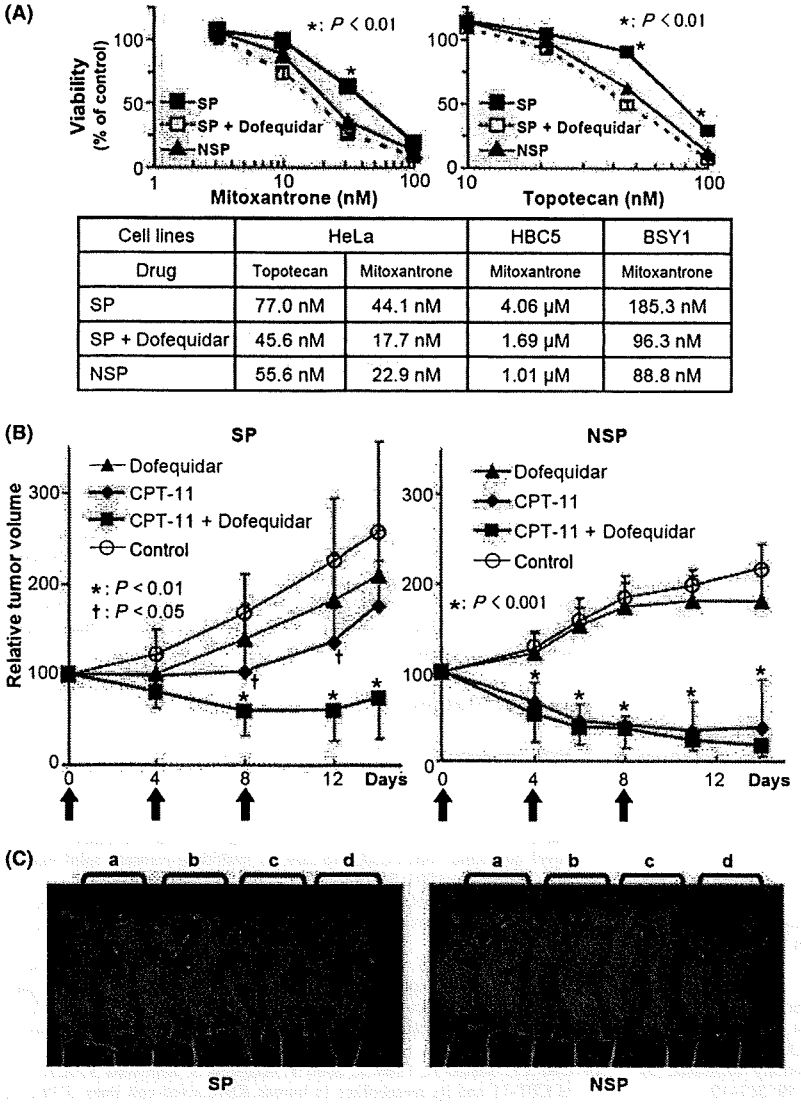

Cell lines	HeLa		HBC5	BSY1
Drug	Topotecan	Mitoxantrone	Mitoxantrone	Mitoxantrone
SP	77.0 nM	44.1 nM	4.06 μM	185.3 nM
SP + Dofequidar	45.6 nM	17.7 nM	1.69 μM	96.3 nM
NSP	55.6 nM	22.9 nM	1.01 μM	88.8 nM

Fig. 6. Sensitization by dofequidar of cancer stem-like SP cells to chemotherapeutic drugs in cells and *in vivo*. (A) SP and NSP cells from HeLa, HBC-5 or BSY-1 cells were cultured in medium containing the indicated concentration of mitoxantrone (upper left panel) or topotecan (upper right panel). In some experiments, side population (SP) cells were cultured in the presence of 3 μM dofequidar (SP+Dofequidar). The lower panel gives a summary of 50% growth inhibition (GI_{50}) values in each experiment. (B) The xenografted HeLa-derived SP and non-SP (NSP) secondary tumors were treated with 200 mg/kg dofequidar, 67 mg/kg CPT-11, or both on days 0, 4, and 8 (arrows) ($n = 6$). Graphs show relative tumor volume. The data of control and CPT-11-treated groups were the same as in Figure 2(D). The xenografted SP tumor size treated with CPT-11 versus control (†) or that treated with CPT-11 plus dofequidar versus control (*) was significantly different ($P < 0.05$ and $P < 0.01$, respectively). (C) The mice bearing HeLa SP (left) or NSP (right) tumors were photographed at 14 days after first treatment. a, Dofequidar-treated; b, CPT-11-treated; c, CPT-11 plus dofequidar-treated; d, control.

clinically relevant model. HeLa-derived SP and NSP cells were transplanted into nude mice, and the xenografted tumors were treated with CPT-11 with or without dofequidar. Dofequidar (200 mg/kg) was orally administrated 30 min before CPT-11 (67 mg/kg) injection. Although xenografted HeLa SP cells showed resistance to CPT-11, co-treatment of the mice with dofequidar drastically decreased the tumor volume (Fig. 6B, left panel), like that seen in CPT-11-treated or CPT-11 plus dofequidar-treated NSP-bearing mice (Fig. 6B, right panel). Dofequidar alone had almost no effect on SP- or NSP-derived tumor growth *in vivo*. To assess the toxicity, we measured the bodyweight of the tumor-bearing mice. The mice seemed to be healthy (Fig. 6C), and the change in bodyweight was very small (data not shown). Thus CPT-11 plus dofequidar therapy appeared to have good therapeutic efficacy *in vivo* by sensitizing cancer stem-like cells to anticancer drugs.

Discussion

It is still difficult to cure advanced cancer with chemotherapy because advanced cancer often shows resistance to many chemotherapeutic agents. Although MDR was thought to result from treatment with chemotherapy,[27] recent studies suggest that the primary tumor already has chemotherapy- or radiation therapy-resistant cells called CSC.[1] Because CSC are able to self-renew and regenerate the tumor, as likely as primary tumor, CSC are thought to be associated with recurrence. Therefore, it is important to study the characteristics of CSC and to develop new therapies targeting them.

In the present study, we used SP cells as a model of cancer stem-like cells. Various cancer cell lines contain SP cells (Fig. 1) that possess the repopulating ability (Fig. 2A). In the breast cancer cell line BSY-1, SP cells have higher cancer-initiating ability than that of NSP cells. Therefore, CSC were concentrated in BSY-1 SP cells (data not shown). On the other hand, both SP and NSP cells from the HeLa cell line could initiate tumor formation after injection of a very few number of cells (Fig. 2C). SP cells, but not NSP cells, from HeLa, however, showed resistance to several anticancer agents (Figs 2D,6A). Therefore, SP cells from cancer cell lines may not always correspond to CSC, but they may, at least, contain more malignant cells.

doi: 10.1111/j.1349-7006.2009.01288.x

To address the targeting of CSC, various efforts have been made, and several studies have reported the success of inducing cell death or differentiation in CSC.[28–32] In the present study, we showed that inhibition of ABC-T by dofequidar was one possible method to overcome anticancer drug resistance in cancer stem-like SP cells *in vitro* and *in vivo* (Figs 5,6).

In human cancer, ABCB1/P-gp, ABCC1/MRP1, and ABCG2/BCRP are the most studied, but there are more ABC-T that relate to cancer. Recently, ABCB5, originally reported to be expressed on the surface of clinically malignant melanoma and a major efflux mediator of doxorubicin in melanoma,[33] marked primitive cells (malignant melanoma-initiating cells) capable of recapitulating melanomas in xenotransplantation models. Further, targeting malignant melanoma-initiating cells with a specific antibody against ABCB5 inhibited tumor growth by inducing antibody-dependent, cell-mediated cytotoxicity.[34] Indeed, it has already been reported that some ABC-T are overexpressed in CSC.[1,7,35] Thus, it is important to understand the characteristics of ABC-T, such as its endogenous substrate, and the mechanisms of ABC-T overexpression in CSC.

From the results of phase III clinical trials of dofequidar for breast cancer patients, dofequidar treatment showed great advances in the patient group of no prior therapy.[17] This result indicates that CSC already existed in primary tumors, and they tended to remain after treatment with anticancer agents alone. Therefore, treating these patients with dofequidar plus conventional chemotherapy might effectively kill the CSC, resulting in good progression-free survival and overall survival in the clinical study. If the CSC remained, they might cause recurrence and might acquire resistance to therapy. Therefore co-administration of a MDR-reversing agent such as dofequidar in primary chemotherapy could drastically reduce the rate of recurrence.

In the present study we used CPT-11 as an anticancer agent in *in vivo* experiments (Figs 2D,6). CPT-11 is one of the most widely prescribed drugs for various cancers, including lung, stomach, colon, and cervical cancer.[18] CPT-11 is a prodrug converted into the active compound SN-38 in the liver. CPT-11 is exported from cells by ABCB1/P-gp and ABCC1/MRP1,[19,20] and the active metabolite SN-38 is exported by ABCG2/BCRP.[21] As dofequidar could inhibit ABCB1/P-gp, ABCC1/MRP1, and ABCG2/BCRP, we tried to treat xenografted tumors with CPT-11 together with dofequidar. From our study, the combination of dofequidar and CPT-11 was shown to be effective in killing of the SP cells *in vivo* without severe side effects (Fig. 6). Dofequidar could have future use as a chemotherapy-sensitizing agent targeting CSC.

Acknowledgments

We thank Drs T. Yamori, A. Tomida, and H. Seimiya for helpful discussions and Ms S. Tsukahara for technical assistance. This study was supported in part by special grants from the Ministry of Education, Culture, Sports, Science, and Technology of Japan, 19790241 and 20015046 (to R. Katayama and N. Fujita, respectively). This study was also supported in part by a grant from the Vehicle Racing Commemorative Foundation and the Mochida Memorial Foundation for Medical and Pharmaceutical Research (to N. Fujita).

Disclosure Statement

No potential conflicts of interest were disclosed.

References

1 Dean M, Fojo T, Bates S. Tumour stem cells and drug resistance. *Nat Rev* 2005; **5**: 275–84.
2 Goodell MA, Brose K, Paradis G, Conner AS, Mulligan RC. Isolation and functional properties of murine hematopoietic stem cells that are replicating *in vivo*. *J Exp Med* 1996; **183**: 1797–806.
3 Zhou S, Schuetz JD, Bunting KD *et al.* The ABC transporter Bcrp1/ABCG2 is expressed in a wide variety of stem cells and is a molecular determinant of the side-population phenotype. *Nat Med* 2001; **7**: 1028–34.
4 Scharenberg CW, Harkey MA, Torok-Storb B. The ABCG2 transporter is an efficient Hoechst 33342 efflux pump and is preferentially expressed by immature human hematopoietic progenitors. *Blood* 2002; **99**: 507–12.
5 Barile L, Messina E, Giacomello A, Marban E. Endogenous cardiac stem cells. *Prog Cardiovasc Dis* 2007; **50**: 31–48.
6 Kato K, Yoshimoto M, Kato K *et al.* Characterization of side-population cells in human normal endometrium. *Hum Reprod* 2007; **22**: 1214–23.
7 Chiba T, Kita K, Zheng YW *et al.* Side population purified from hepatocellular carcinoma cells harbors cancer stem cell-like properties. *Hepatology* 2006; **44**: 240–51.
8 Haraguchi N, Utsunomiya T, Inoue H *et al.* Characterization of a side population of cancer cells from human gastrointestinal system. *Stem Cells* 2006; **24**: 506–13.
9 Hirschmann-Jax C, Foster AE, Wulf GG *et al.* A distinct "side population" of cells with high drug efflux capacity in human tumor cells. *Proc Natl Acad Sci USA* 2004; **101**: 14 228–33.
10 Kondo T, Setoguchi T, Taga T. Persistence of a small subpopulation of cancer stem-like cells in the C6 glioma cell line. *Proc Natl Acad Sci USA* 2004; **101**: 781–6.
11 Tsuruo T, Iida H, Tsukagoshi S, Sakurai Y. Overcoming of vincristine resistance in P388 leukemia in vivo and in vitro through enhanced cytotoxicity of vincristine and vinblastine by verapamil. *Cancer Res* 1981; **41**: 1967–72.
12 Szakacs G, Paterson JK, Ludwig JA, Booth-Genthe C, Gottesman MM. Targeting multidrug resistance in cancer. *Nat Rev Drug Discov* 2006; **5**: 219–34.
13 Suzuki T, Fukazawa N, San-nohe K, Sato W, Yano O, Tsuruo T. Structure-activity relationship of newly synthesized quinoline derivatives for reversal of multidrug resistance in cancer. *J Med Chem* 1997; **40**: 2047–52.
14 Naito M, Matsuba Y, Sato S, Hirata H, Tsuruo T. MS-209, a quinoline-type reversal agent, potentiates antitumor efficacy of docetaxel in multidrug-resistant solid tumor xenograft models. *Clin Cancer Res* 2002; **8**: 582–8.
15 Nakanishi O, Baba M, Saito A *et al.* Potentiation of the antitumor activity by a novel quinoline compound, MS-209, in multidrug-resistant solid tumor cell lines. *Oncol Res* 1997; **9**: 61–9.
16 Sato W, Fukazawa N, Nakanishi O *et al.* Reversal of multidrug resistance by a novel quinoline derivative, MS-209. *Cancer Chemother Pharmacol* 1995; **35**: 271–7.
17 Saeki T, Nomizu T, Toi M *et al.* Dofequidar fumarate (MS-209) in combination with cyclophosphamide, doxorubicin, and fluorouracil for patients with advanced or recurrent breast cancer. *J Clin Oncol* 2007; **25**: 411–17.
18 Rothenberg ML. Topoisomerase I inhibitors: review and update. *Ann Oncol* 1997; **8**: 837–55.
19 Chu XY, Suzuki H, Ueda K, Kato Y, Akiyama S, Sugiyama Y. Active efflux of CPT-11 and its metabolites in human KB-derived cell lines. *J Pharmacol Exp Ther* 1999; **288**: 735–41.
20 Jansen WJ, Hulscher TM, van Ark-Otte J, Giaccone G, Pinedo HM, Boven E. CPT-11 sensitivity in relation to the expression of P170-glycoprotein and multidrug resistance-associated protein. *Br J Cancer* 1998; **77**: 359–65.
21 Kawabata S, Oka M, Shiozawa K *et al.* Breast cancer resistance protein directly confers SN-38 resistance of lung cancer cells. *Biochem Biophys Res Commun* 2001; **280**: 1216–23.
22 Kage K, Tsukahara S, Sugiyama T *et al.* Dominant-negative inhibition of breast cancer resistance protein as drug efflux pump through the inhibition of S-S dependent homodimerization. *Int J Cancer* 2002; **97**: 626–30.
23 Narasaki F, Oka M, Fukuda M *et al.* A novel quinoline derivative, MS-209, overcomes drug resistance of human lung cancer cells expressing the multidrug resistance-associated protein (MRP) gene. *Cancer Chemother Pharmacol* 1997; **40**: 425–32.
24 Rabindran SK, Ross DD, Doyle LA, Yang W, Greenberger LM. Fumitremorgin C reverses multidrug resistance in cells transfected with the breast cancer resistance protein. *Cancer Res* 2000; **60**: 47–50.
25 Mao Q, Unadkat JD. Role of the breast cancer resistance protein (ABCG2) in drug transport. *AAPS J* 2005; **7**: E118–33.
26 Allen JD, van Loevezijn A, Lakhai JM *et al.* Potent and specific inhibition of the breast cancer resistance protein multidrug transporter in vitro and in mouse intestine by a novel analogue of fumitremorgin C. *Mol Cancer Ther* 2002; **1**: 417–25.
27 Borst P, Evers R, Kool M, Wijnholds J. A family of drug transporters: the multidrug resistance-associated proteins. *J Natl Cancer Inst* 2000; **92**: 1295–302.
28 Jordan CT, Guzman ML, Noble M. Cancer stem cells. *N Engl J Med* 2006; **355**: 1253–61.

29 Ito K, Bernardi R, Morotti A *et al.* PML targeting eradicates quiescent leukaemia-initiating cells. *Nature* 2008; **453**: 1072–8.
30 Jin L, Hope KJ, Zhai Q, Smadja-Joffe F, Dick JE. Targeting of CD44 eradicates human acute myeloid leukemic stem cells. *Nat Med* 2006; **12**: 1167–74.
31 Li L, Neaves WB. Normal stem cells and cancer stem cells: the niche matters. *Cancer Res* 2006; **66**: 4553–7.
32 Piccirillo SG, Reynolds BA, Zanetti N *et al.* Bone morphogenetic proteins inhibit the tumorigenic potential of human brain tumour-initiating cells. *Nature* 2006; **444**: 761–5.
33 Frank NY, Margaryan A, Huang Y *et al.* ABCB5-mediated doxorubicin transport and chemoresistance in human malignant melanoma. *Cancer Res* 2005; **65**: 4320–33.
34 Schatton T, Murphy GF, Frank NY *et al.* Identification of cells initiating human melanomas. *Nature* 2008; **451**: 345–9.
35 Ho MM, Ng AV, Lam S, Hung JY. Side population in human lung cancer cell lines and tumors is enriched with stem-like cancer cells. *Cancer Res* 2007; **67**: 4827–33.

Supporting Information

Additional supporting information may be found in the online version of this article:

Fig. S1. Dofequidar inhibits ABCG2/BCRP in addition to ABCB1.

Table S1. Sequence information of qRT-PCR primers and siRNA for ABCG2.

Please note: Wiley-Blackwell are not responsible for the content or functionality of any supporting materials supplied by the authors. Any queries (other than missing material) should be directed to the corresponding author for the article.

doi: 10.1111/j.1349-7006.2009.01288.x

Cancer Science
The official journal of the Japanese Cancer Association

Substrate-dependent bidirectional modulation of P-glycoprotein-mediated drug resistance by erlotinib

Kohji Noguchi,[1] Haruka Kawahara,[1] Airi Kaji,[1] Kazuhiro Katayama,[1] Junko Mitsuhashi[1,2] and Yoshikazu Sugimoto[1,2,3]

[1]Division of Chemotherapy, Graduate School of Pharmaceutical Sciences, Keio University, Minato-ku, Tokyo; [2]Division of Gene Therapy, Cancer Chemotherapy Center, Japanese Foundation for Cancer Research, Koto-ku, Tokyo, Japan

(Received January 7, 2009/Revised April 24, 2009/Accepted May 3, 2009/Online publication May 31, 2009)

Epidermal growth factor receptor tyrosine kinase inhibitors (EGFR-TKIs) inhibit the function of certain adenosine triphosphate (ATP)-binding cassette transporters, including P-glycoprotein/ABCB1 and breast cancer resistance protein (BCRP)/ABCG2. We previously reported an antagonistic activity of gefitinib towards BCRP. We have now analyzed the effects of erlotinib, another EGFR-TKI, on P-glycoprotein and BCRP. As with gefitinib, erlotinib effectively reversed BCRP-mediated resistance to SN-38 (7-ethyl-10-hydroxycamptothecin) and mitoxantrone. In contrast, we found that erlotinib effectively suppressed P-glycoprotein-mediated resistance to vincristine and paclitaxel, but did not suppress resistance to mitoxantrone and doxorubicin. Conversely, erlotinib appeared to enhance P-glycoprotein-mediated resistance to mitoxantrone in K562/MDR cells. This bidirectional activity of erlotinib was not observed with verapamil, a typical P-glycoprotein inhibitor. Flow cytometric analysis showed that erlotinib co-treatment restored intracellular accumulation of mitoxantrone in K562 cells expressing BCRP, but not in cells expressing P-glycoprotein. Consistently, erlotinib did not inhibit mitoxantrone efflux in K562/MDR cells although it did vincristine efflux in K562/MDR cells and mitoxantrone efflux in K562/BCRP cells. Intravesicular transport assay showed that erlotinib inhibited both P-glycoprotein-mediated vincristine transport and BCRP-mediated estrone 3-sulfate transport. Intriguingly, Lineweaver-Burk plot suggested that the inhibitory mode of erlotinib was a mixed type for P-glycoprotein-mediated vincristine transport whereas it was a competitive type for BCRP-mediated estrone 3-sulfate transport. Collectively, these observations indicate that the pharmacological activity of erlotinib on P-glycoprotein-mediated drug resistance is dependent upon the transporter substrate. These findings will be useful in understanding the pharmacological interactions of erlotinib used in combinational chemotherapy. (*Cancer Sci* 2009; 100: 1701–1707)

The ABC transporter protein P-glycoprotein/ABCB1 consists of two symmetrical halves connected by a linker region, with each half containing an ATP-binding domain and a six transmembrane domain.[1] P-glycoprotein has been investigated as a key cancer-related protein whose overexpression can lead to a tumor cell multidrug resistant phenotype.[1] P-glycoprotein transports out of cells various structurally unrelated chemotherapeutic agents, including vincristine (VCR), paclitaxel (PTX), doxorubicin (DOX), and mitoxantrone (MXR), thereby reducing their cytotoxic effects.[1] Overexpression of breast cancer resistance protein (BCRP)/ABCG2, a half-type ABC transporter with an ATP-binding domain and a six transmembrane domain, also modulates the efficacy of cancer chemotherapeutics,[2] rendering cancer cells resistant to various chemotherapeutic drugs. BCRP functions as a homodimer, transporting anticancer agents such as topotecan, irrinotecan, SN-38 (7-ethyl-10-hydroxycamptothecin), methotrexate, and MXR out of cells.[3]

A number of compounds have been tested for their ability to overcome ABC transporter-mediated drug resistance. Verapamil, cyclosporine A, and others have been identified as inhibitors of P-glycoprotein,[1,4,5] while fumitremorgin C (FTC), tamoxifen derivatives, and certain flavonoids inhibit BCRP.[3,6–8] These reagents directly interact with P-glycoprotein or BCRP and competitively interfere with transporter-substrate binding. This inhibition restores intracellular accumulation of the substrate drugs, effectively reversing drug resistance.

Epidermal growth factor receptor (EGFR) is a member of the ErbB/HER family of receptor tyrosine kinases and is frequently deregulated in human cancers, including non-small cell lung cancer (NSCLC), breast cancer, and glioblastomas.[9] As such, abnormal activation of EGFR signaling is a promising therapeutic target. Gefitinib and erlotinib, both EGFR inhibitory 4-anilinoquinazoline derivatives, are currently utilized in clinical chemotherapy, especially for lung cancer.[10] Extensive examination of functional interactions between BCRP and imatinib or gefitinib revealed that these kinase inhibitors are also substrates for BCRP with potent inhibitory activity against this ABC transporter.[11,12]

Erlotinib is an orally active EGFR tyrosine kinase inhibitor (TKI) with efficacy in NSCLC, ovarian cancer, pancreatic cancer, head and neck squamous cell cancer, and primary glioblastoma.[13] Erlotinib is approved in the United States for treatment of locally advanced or metastatic NSCLC after failure of at least one prior chemotherapy regimen.[14] It was also recently approved for use in combination with gemcitabine as a first line treatment for patients with locally advanced, unresectable, or metastatic pancreatic cancer.[15] Several clinical studies are planned to examine the combinational effects of erlotinib or gefitinib on conventional chemotherapy with various tumors. Detailed exploration of the pharmacological interaction between erlotinib and anticancer agents will contribute to optimize synergistic effects in such combination chemotherapy. Most recently, Shi *et al.* reported that erlotinib antagonized both P-glycoprotein- and BCRP-mediated drug resistances through direct inhibition of their efflux activities.[16,17] In the present study, we demonstrate that erlotinib inhibition of P-glycoprotein activity is substrate-specific.

Materials and Methods

Reagents. Erlotinib was kindly provided by F. Hoffmann-La Roche (Basel, Switzerland). SN-38 was provided by Yakult Honsha (Tokyo, Japan). FTC was purchased from Alexis (San Diego, CA, USA) and verapamil was purchased from Sigma-Aldrich (St. Louis, MO, USA). All other anticancer drugs were commercially available. MTT (3-[4,5-dimethyl-2-thiazolyl]-2,5-diphenyl-2H-tetrazolium bromide) was obtained from Wako Pure Chemical Industries, (Osaka, Japan).

Cells and drug sensitivity assay. PC-9 human NSCLC cells and K562 human myelogenous leukemia cells were cultured in DMEM and RPMI-1640 mediums, respectively, supplemented

[3]To whom correspondence should be addressed.
E-mail: sugimoto-ys@pha.keio.ac.jp

doi: 10.1111/j.1349-7006.2009.01213.x

with 7% fetal bovine serum and kanamycin (50 μg/mL) at 37 °C in a 5% CO_2 atmosphere. BCRP-expressing K562 cells (K562/BCRP), P-glycoprotein-expressing K562 cells (K562/MDR), and BCRP-expressing PC-9 cells (PC-9/BCRP) were established previously.[2] PC-9/MDR cells were established by the transduction of PC-9 with a HaMDR retrovirus harboring a Myc-tagged human *MDR1* cDNA in the Ha retrovirus vector as described previously.[18]

Erlotinib-induced growth inhibition of PC-9 and K562 cell lines was determined using a Coulter counter as described previously.[8] The effects of erlotinib on cell sensitivity to anticancer drugs were evaluated by MTT assay. Briefly, cells were seeded at 2×10^3 cells/well in 96-well plates. After incubation at 37 °C for 5 days in the presence of various concentrations of the drugs, MTT solution was added into each well and incubated for 4 h. An SDS/HCl solution was then added and incubated overnight to dissolve the formazan precipitate. Finally, OD570 was measured to estimate cell growth. IC_{50} values (the dosage of drug at which a 50% inhibition of cell growth was achieved) were determined from the growth inhibition curve. Reversal indices (RI50) were defined as the concentration of inhibitors (erlotinib, verapamil or FTC) that caused a 2-fold reduction in the IC_{50} values for anticancer drugs in each resistant cell as described previously.[8]

Intracellular accumulation of mitoxantrone. The effect of erlotinib on the cellular accumulation of MXR was determined by flow cytometry. K562, K562/BCRP, and K562/MDR cells (5×10^5 cells each) were incubated with 300 nmol/L MXR at 37 °C for 40 min in the absence or presence of erlotinib (0.1, 1, and 10 μmol/L), verapamil (1 and 10 μmol/L), or FTC (1 and 10 μmol/L). Cells were then washed with ice-cold PBS and subjected to fluorescence analysis using a BD LSR II system (Becton Dickinson, San Jose, CA, USA). MXR fluorescence was measured using a red 633-nm laser and a 660/20-band pass filter.

Intravesicular transport assay. Membrane vesicles of K562/MDR cells were prepared according to the method described previously.[19] The vesicular transport assay was done by a rapid centrifugation technique using ^{3}H-labeled VCR, MXR (American Radiolabeled Chemicals, St. Louis, MO, USA) and estrone 3-sufate (E1S) (Perkin-Elmer Life Sciences, Boston, MA, USA) as essentially described before.[12] In brief, the transport reaction mixture (50 μL volume; 50 mmol/L Tris-HCl [pH 7.4], 10 mmol/L $MgCl_2$, 250 mmol/L sucrose, 10 mmol/L phosphocreatine, 100 μg/mL creatine phosphokinase, with or without 3 mmol/L ATP, 100 nmol/L [^{3}H]VCR or 50 nmol/L [^{3}H]E1S, and membrane vesicles containing 10 μg protein) was kept on ice for 5 min and then reaction was started by incubation at 25 °C for 10 min. The reaction was terminated by an addition of 1 mL of ice-cold stop solution (10 mmol/L Tris-HCl [pH 7.4], 100 mmol/L NaCl, 250 mmol/L sucrose). The membrane vesicles were collected by centrifugation at 18 000 *g* for 10 min at 4 °C. The pellets were solubilized to measure their radioactivity levels by a liquid scintillation counter.

Cellular efflux assay. Cells (10^6/mL) were incubated with 0.2 μmol/L ^{3}H-labeled MXR or VCR for 30 min at 37 °C, washed twice with ice-cold PBS, and then suspended in ice-cold ^{3}H-free fresh normal growth medium. Aliquots of them were immediately mixed with ice-cold growth medium containing inhibitor (10 μmol/L each), stood in ice-water for 5 min, and then incubated at 37 °C for indicated times. Cell suspensions were centrifuged at 800 *g* for 5 min, and supernatants were collected to measure [^{3}H] radioactivity levels exported from cells by a liquid scintillation counter.

Results

Breast cancer resistance protein (BCRP)-mediated erlotinib resistance in PC-9 cells but not in K562 cells. The NSCLC cell line PC-9 harbors an *EGFR* gene with a 15-bp deletion[20] and shows enhanced sensitivity to the EGFR inhibitor gefitinib. K562 cells, on the other hand, express very little EGFR and do not show selective sensitivity to gefitinib inhibition.[12] We have observed that BCRP transports gefitinib and confers resistance to gefitinib only in gefitinib-sensitive cells such as PC-9, but not in non-sensitive cells such as K562.[2]

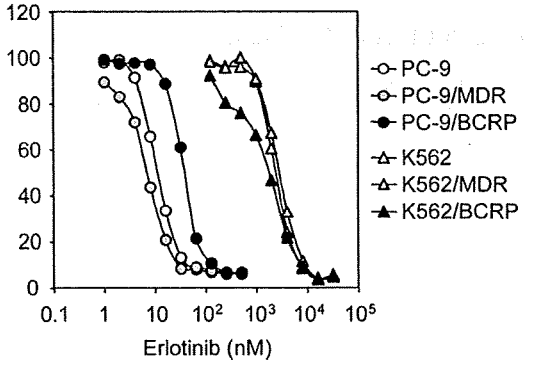

Fig. 1. Sensitivity of PC-9 and K562 cell lines to erlotinib. Cells were cultured for 5 days with increasing concentrations of erlotinib. Cell numbers were determined with a Coulter counter and cell growth inhibition curves (% of control) are shown. Data points are means ± SD calculated from triplicate determinations. Different symbols indicate specific cell lines: PC-9, open circles; PC-9/MDR, shaded circles; PC-9/breast cancer resistance protein (BCRP), filled circles; K562, open triangles; K562/MDR, shaded triangles; and K562/BCRP, filled triangles.

Sensitivity to erlotinib, another EGFR-TKI, was characterized in PC-9 and K562 cells expressing P-glycoprotein or BCRP (PC-9/MDR, PC-9/BCRP, K562/MDR, and K562/BCRP). Cells were incubated with erlotinib and the ratio of cell growth inhibition was used to determine IC_{50} values for each cell line. As shown in Figure 1, erlotinib inhibited PC-9 cell growth at nanomoler concentrations (IC_{50}, ~10 nmol/L), whereas K562 cells grew normally in the presence of such lower concentrations of erlotinib (IC_{50}, 2.4 μmol/L). Thus, PC-9 cells were more sensitive to erlotinib than K562 cells. Interestingly, PC-9/BCRP cells were approximately 2.8-fold more resistant to erlotinib than parental PC-9 and PC-9/MDR cells. The sensitivity of K562/MDR or K562/BCRP cells in erlotinib was almost identical to that of the parental K562 cells. Consistent with the published results for gefitinib,[12] the present findings indicate that BCRP expression confers resistance to erlotinib in PC-9 cells but not in K562 cells.

Effects of erlotinib on BCRP-mediated drug resistance. Gefitinib acts as an inhibitor for transporters and reverses P-glycoprotein- and BCRP-mediated resistance to various anticancer drugs.[12] K562 cells were not sensitive to the selective cytotoxicity of erlotinib-mediated EGFR inhibition. Therefore, we used K562/MDR and K562/BCRP cell lines to test such erlotinib reversal activity affecting P-glycoprotein- and BCRP-mediated drug resistance. K562/BCRP cells showed significant resistance to SN-38 (~25-fold) and MXR (~7-fold). Erlotinib co-treatment effectively reversed BCRP-mediated resistance to both drugs (Fig. 2a,b).

The dose dependency of this erlotinib-mediated suppressive effect was also analyzed. Erlotinib at 1.5 μmol/L (Fig. 2, open squares) effectively eliminated BCRP-mediated resistance to SN-38 and MXR. In similar experiments using erlotinib or FTC as a control inhibitor of BCRP-mediated resistance, both drugs reduced resistance to SN-38 and MXR in a dose-dependent manner (Fig. 2c,d). BCRP-mediated drug resistance reversal abilities for erlotinib and FTC were calculated as the RI50 value that caused a 2-fold reduction in the IC_{50} for each drug. As

doi: 10.1111/j.1349-7006.2009.01213.x

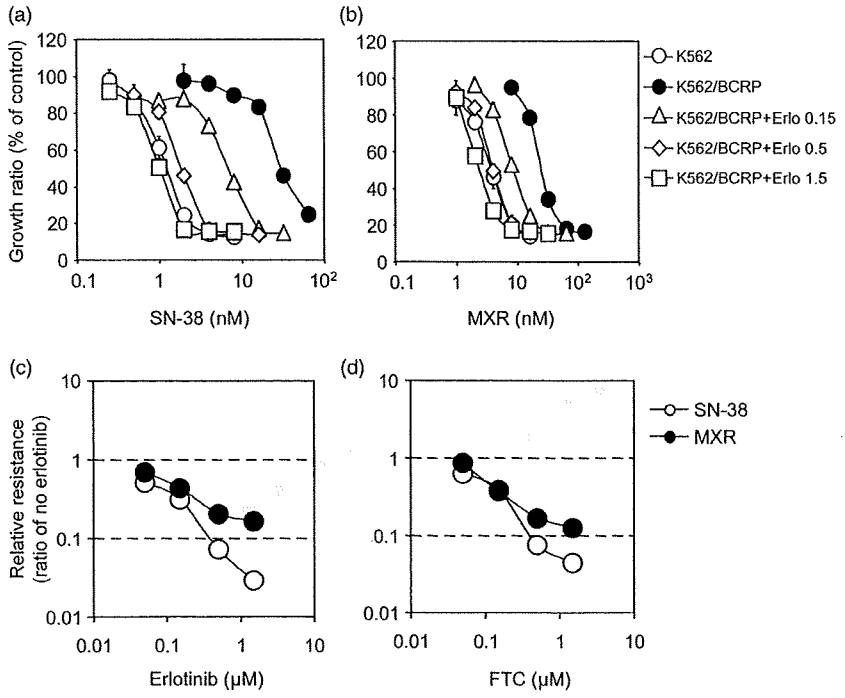

Fig. 2. Reversal of breast cancer resistance protein (BCRP)-mediated drug resistance in K562/BCRP cells. The sensitivity of K562/BCRP cells to SN-38 (7-ethyl-10-hydroxycamptothecin) (a) and mitoxantrone (MXR) (b) was determined in the presence of different concentrations of erlotinib: 0.15 μmol/L, open triangles; 0.5 μmol/L, open diamonds; 1.5 μmol/L, open squares. Cell growth inhibition following 5 days of culture was determined using the MTT assay. Growth inhibition curves were established from the means ± SD of triplicate determinations. Similar experiments were performed in the presence of fumitremorgin C (FTC) and the relative resistance to SN-38 (open circles) or MXR (filled circles) in the presence erlotinib (c) or FTC (d) was calculated as the ratio of an IC_{50} value in the presence of an inhibitor divided by the IC_{50} value without inhibitors.

Table 1. Values of RI50 (μM) to BCRP-mediated resistance

		Erlotinib	FTC
BCRP	MXR	0.10 ± 0.01	0.19 ± 0.02
	SN-38	0.05 ± 0.01	0.09 ± 0.02

Means ± SD. Experiments were performed in triplicate.
BCRP, breast cancer resistance protein; FTC, fumitremorgin C; MXR, mitoxantrone; RI50, reversal indices; SN-38, 7-ethyl-10-hydroxycamptothecin.

shown in Table 1, the RI50 values of erlotinib to SN-38 and MXR were 0.05 and 0.1 μmol/L, respectively. Interestingly, SN-38 resistance was more susceptible to erlotinib than MXR resistance. The RI50 values of erlotinib were comparable with those of FTC. Thus, erlotinib and FTC appeared to have equivalent inhibitory activities against BCRP-mediated drug resistance.

Distinct modulation of P-glycoprotein-mediated drug resistance by erlotinib. Although our experiments did not show obvious erlotinib-resistance in PC-9/MDR cells, we examined the effects of erlotinib on P-glycoprotein-mediated drug resistance in K562 cells based on reports that gefitinib was able to reverse P-glycoprotein-mediated drug resistance. MTT assays showed that K562/MDR cells were resistant to VCR (relative resistance was ~360-fold), PTX (~1000-fold), DOX (~25-fold), and MXR (~9-fold) (data not shown). We next examined the effects of erlotinib at various concentrations. Representative results showing K562/MDR cell resistance to VCR and to MXR are presented in Figure 3(a,b). As previously reported for gefitinib,[12] erlotinib effectively reversed VCR-resistance in K562/MDR cells (Fig. 3a). However, when K562/MDR cells were co-treated with erlotinib at 1.5 μmol/L, cells still showed significant resistance to VCR (~32-fold, open squares), whereas erlotinib completely eliminated BCRP-mediated resistance to SN-38 (as shown in Fig. 2a). Higher concentrations of erlotinib (over 5 μmol/L) were required for complete reversal of P-glycoprotein-mediated VCR-resistance. Moreover, we unexpectedly found that in K562/MDR cells, erlotinib did not reverse resistance to MXR. Conversely, erlotinib at concentrations of 0.15–1.5 μmol/L shifted the growth inhibition curve to the right (Fig. 3b), suggesting that erlotinib treatment stimulated P-glycoprotein-mediated resistance to MXR.

Variations in IC_{50} values for co-treatments with erlotinib or verapamil and each anticancer drug were determined in order to compare their ability to inhibit P-glycoprotein-mediated resistance phenotypes (Fig. 3c,d). This assessment showed that verapamil, a typical MDR-inhibitor, actually suppressed resistance to a series of drugs (VCR, PTX, DOX, and MXR) mediated by P-glycoprotein at similar concentrations (Fig. 3d). In contrast, erlotinib-induced reversal of P-glycoprotein-mediated resistance was different for individual anticancer drugs. Co-treatment of K562/MDR cells with erlotinib at 1.5 μmol/L, which significantly suppressed resistance to both VCR and PTX (Fig. 3c, open squares and open diamonds respectively), did not affect resistance to DOX (Fig. 3c, filled triangles). Thus, the P-glycoprotein-mediated resistance to DOX was less sensitive to erlotinib-mediated inhibition compared with resistance to VCR.

Remarkably, resistance to MXR was hardly affected by erlotinib, even at 5 μmol/L. Conversely, erlotinib co-treatment (0.15–1.5 μmol/L) increased MXR resistance in K562/MDR cells (Fig. 3c, filled circles). We confirmed these bidirectional effects of erlotinib on P-glycoprotein-mediated resistance with two different methods: the MTT assay and a cell growth assay that counted cell numbers using a Coulter counter (data not shown). Both methods suggested that at clinical concentrations, erlotinib potentiated P-glycoprotein-mediated resistance to MXR in K562/MDR cells.

As shown in Table 2, calculated RI50 values of erlotinib treatment for P-glycoprotein-mediated resistance to each anticancer drug clearly showed that P-glycoprotein-mediated resistance to DOX and MXR was approximately 10-fold less sensitive to erlotinib than observed for VCR and PTX. Conversely, verapamil reversed resistance to each of these drugs at comparable concentrations (RI50, 0.11–0.18 μmol/L). Therefore, the effects of erlotinib on P-glycoprotein-mediated resistance were quite different from those observed for verapamil and also from erlotinib

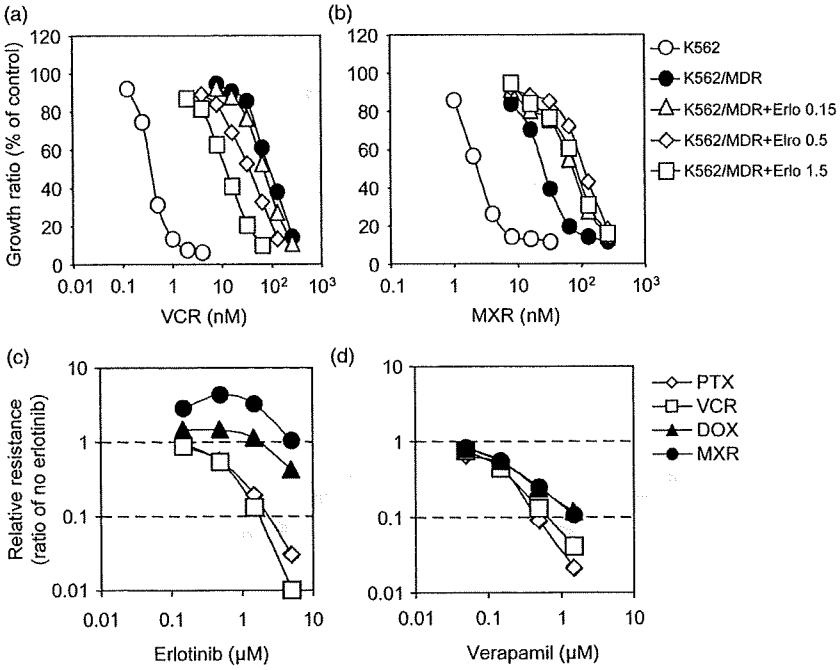

Fig. 3. Reversal of P-glycoprotein-mediated drug resistance in K562/MDR cells. The sensitivity of K562/MDR cells to vincristine (VCR) (a) and mitoxantrone (MXR) (b) was determined in the presence of different concentrations of erlotinib: 0.15 μmol/L, open triangles; 0.5 μmol/L, open diamonds; 1.5 μmol/L, open squares. The sensitivity of K562 (open circles) and K562/MDR (filled circles) cells to VCR (a) and MXR (b) was also determined in the absence of erlotinib. Cell growth inhibition following 5 days of culture was determined using the MTT assay. Growth inhibition curves were established from the means ± SD of triplicate determinations. Similar cell growth inhibition assays were performed using paclitaxel (PTX) and doxorubicin (DOX) in the presence of erlotinib or verapamil (0.05, 0.15, 0.5, and 1.5 μmol/L). Relative resistance to PTX (open diamonds), VCR (open squares), DOX (filled triangles), and MXR (filled circles) in the presence erlotinib (c) or verapamil (d) were calculated as the ratio of an IC_{50} value in the presence of an inhibitor divided by the IC_{50} value without inhibitors.

Table 2. Values of RI50 (μM) to P-glycoprotein-mediated resistance

		Erlotinib	Verapamil
MDR	MXR	–	0.18 ± 0.01
	DOX	4.0 ± 0.2	0.18 ± 0.01
	VCR	0.37 ± 0.02	0.11 ± 0.02
	PTX	0.44 ± 0.02	0.13 ± 0.03

Means ± SD. Experiments were performed in triplicate.
DOX, doxorubicin; MXR, mitoxantrone; PTX, paclitaxel; RI50, reversal indices; VCR, vincristine.

effects on BCRP-mediated resistance. Collectively, these data indicated that inhibitory ability of erlotinib was dependent upon the specific substrate in the P-glycoprotein-mediated resistance phenotype.

Effects of erlotinib on intracellular accumulation of mitoxantrone in cells expressing ABC transporters. The observations described above suggest that erlotinib may inhibit cellular efflux of MXR mediated by the ABC transporter BCRP, but not by P-glycoprotein. The effects of erlotinib on the intracellular accumulation of MXR in BCRP- or P-glycoprotein-expressing K562 cells were examined by flow cytometric analysis. After incubating cells with 300 nmol/L MXR for 40 min, fluorescence intensity indicative of MXR uptake significantly increased in K562/BCRP and K562/MDR cells (Fig. 4a,b). These results indicated that BCRP and P-glycoprotein exported MXR out of the cells.

Erlotinib co-treatment enhanced MXR cellular fluorescence intensity in K562/BCRP cells in a dose-dependent manner (Fig. 4c). The intracellular accumulation levels of MXR were determined by measuring peak fluorescence values at each point to compare efficacies of each inhibitor (Fig. 4e, with K562/BCRP cells shown as open columns). FTC or erlotinib at 10 μmol/L caused a similar enhancement of MXR accumulation in K562/BCRP cells, suggesting that erlotinib suppressed MXR efflux through BCRP with an efficacy that was similar to FTC.

Next, similar experiments were performed in K562/MDR cells to determine whether erlotinib modulates P-glycoprotein-mediated MXR transport (Fig. 4d). Consistent with its other effects on the P-glycoprotein-mediated resistance phenotype, co-treatment with erlotinib at concentrations up to 10 μmol/L did not enhance MXR fluorescence intensity in K562/MDR cells (Fig. 4d,e). Instead, erlotinib at 0.1–1 μmol/L slightly reduced MXR fluorescence intensity, suggesting that erlotinib treatment stimulated the MXR efflux mediated by P-glycoprotein. This effect of erlotinib on P-glycoprotein was in agreement with a stimulation of MXR resistance by erlotinib co-treatment in K562/MDR cells (Fig. 3b). Taken together, these results indicate that erlotinib suppressed MXR efflux mediated by BCRP, but not by P-glycoprotein, in K562 cells.

Effects of erlotinib on P-glycoprotein-mediated transport. Next we examined an effect of erlotinib on cellular efflux of VCR and MXR in K562/MDR and K562/BCRP cells (Fig. 5). Time course–dependent extracellular accumulations of [^{3}H]VCR in the supernatants of K562/MDR cell samples were clearly suppressed by both erlotinib and verapamil at 10 μmol/L (Fig. 5a, closed and open circles respectively). These data indicated that P-glycoprotein-mediated VCR efflux was inhibited by erlotinib. However, similar experiments using MXR as a transporter substrate showed that erlotinib did not inhibit MXR efflux in K562/MDR cells (Fig. 5b) despite the fact that erlotinib suppressed BCRP-mediated MXR efflux like FTC (Fig. 5c). These observations indicated that erlotinib sensitivity of P-glycoprotein was dependent on the transporter substrate type.

To understand the possible mechanism for substrate-dependent erlotinib inhibition on P-glycoprotein, intravesicular transport assay was performed to analyze kinetics of erlotinib inhibition on P-glycoprotein-mediated drug transport *in vitro* using membrane vesicles from K562/MDR cells. As shown in Figure 6a, ATP-dependent [^{3}H]VCR transport was actually inhibited by erlotinib in a dose-dependent manner, although with less efficiency than by verapamil (IC_{50} values of erlotinib and verapamil were 2 and 0.2 μmol/L respectively). Moreover, Lineweaver-Burk plot analysis showed that the inhibitory mode of erlotinib for P-glycoprotein-mediated VCR transport was a mixed type while

doi: 10.1111/j.1349-7006.2009.01213.x

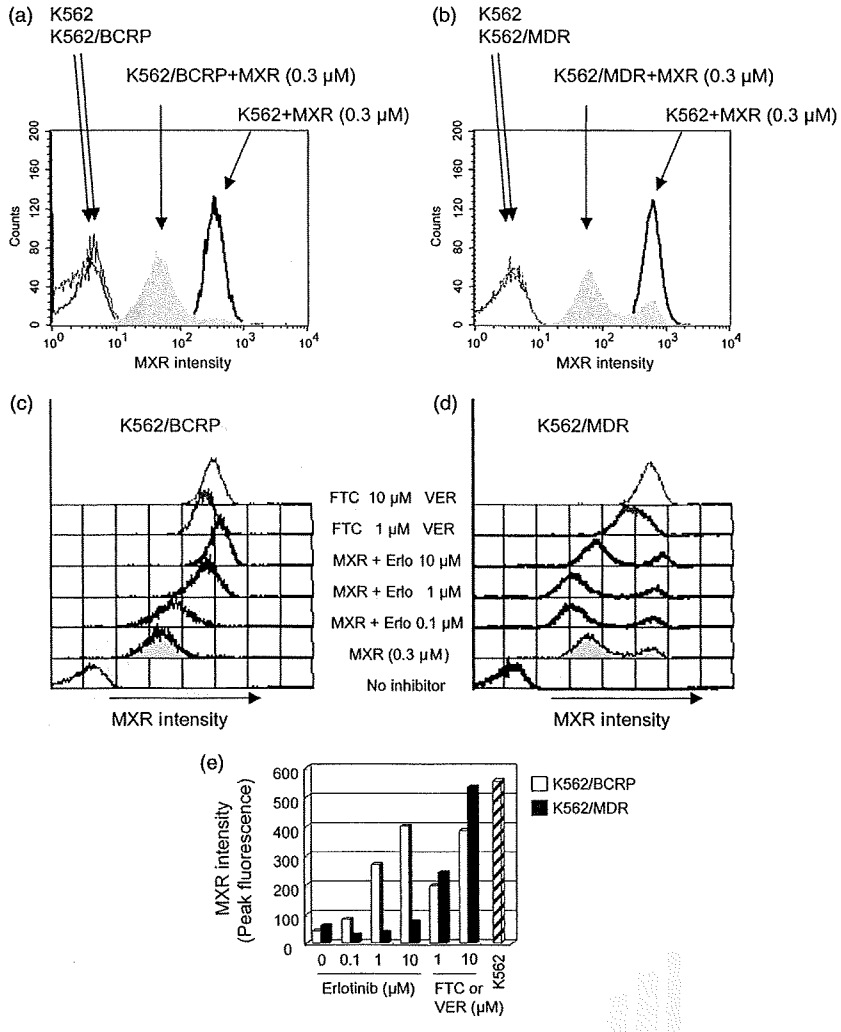

Fig. 4. Effects of erlotinib on the intracellular accumulation of MXR. Breast cancer resistance protein (BCRP)- and P-glycoprotein-mediated efflux reduces intracellular accumulation of mitoxantrone (MXR) (a and b). K562, K562/BCRP (a), and K562/MDR (b) cells were incubated for 40 min in the absence or presence of 0.3 μmol/L MXR, and then washed as described in 'Materials and Methods'. Cellular uptake of MXR was determined as fluorescence intensity of MXR measured by flow cytometry. Modulation of MXR accumulation by erlotinib (c and d). K562/BCRP (c) and K562/MDR (d) cells were incubated with MXR (0.3 μmol/L) and inhibitory agents, erlotinib (0, 0.1, 1, and 10 μmol/L) or the selective inhibitor fumitremorgin C (FTC) (c, shaded lines) or verapamil (VER) (d, shaded lines) at 1 and 10 μmol/L for 40 min. Cellular uptake of MXR was measured as described above, and MXR levels were determined as peak fluorescence values. Intracellular MXR accumulation patterns are shown as change of peak fluorescence values (e). A peak fluorescence for K562 cells is shown as control (slash column).

that of verapamil was a competitive type (Fig. 6b). The calculated *Vmax* values (pmol/mg/min) were 18 in control, 1.8 in erlotinib (2 μmol/L)-treated, and 17.8 in verapamil (0.2 μmol/L)-treated samples respectively, and the calculated *Ki* value of verapamil was 270 nmol/L.

The erlotinib effect on BCRP was also analyzed using membrane vesicles from K562/BCRP cells and [^{3}H]estrone 3-sulfate (E1S) as a transporter substrate of BCRP in an *in vitro* system. These experiments showed that both erlotinib and FTC inhibited BCRP-mediated E1S transport with similar efficiency (IC_{50} values of erlotinib and FTC were 0.13 and 0.25 μmol/L respectively) (Fig. 6c). In this case, Lineweaver-Burk plot analysis indicated that the calculated *Vmax* values (pmol/mg/min) in control, erlotinib (0.13 μmol/L)-treated, and FTC (0.25 μmol/L)-treated samples appeared to be at similar levels (20 in control, 18.9 in erlotinib treated, and 19.5 in FTC-treated, respectively). The calculated *Ki* value of erlotinib was about 150 nmol/L and that of FTC was about 550 nmol/L to BCRP-mediated E1S transport. Therefore, the inhibitory mode of erlotinib for BCRP-mediated E1S transport looked a competitive type (Fig. 6d), which was different from that for P-glycoprotein-mediated VCR transport. Our data also suggested that erlotinib has stronger inhibitory activity to BCRP than FTC. Collectively, these results indicated that the inhibitory mechanism of erlotinib on the transporter function of P-glycoprotein seemed different from that on the BCRP function.

Discussion

We have previously shown functional interplay between gefitinib and BCRP[12] which suggested gefitinib as a competitor for other BCRP substrates, including SN-38 and MXR. In the present study, we further demonstrated that erlotinib modulated BCRP-mediated drug resistance and efflux at sub-micromoler concentrations like a competitive inhibitor. Conversely, we found that erlotinib had only minimal effects on P-glycoprotein-mediated drug resistance to MXR and DOX, and even potentiated MXR resistance in K562/MDR cells at concentrations of 0.15–1.5 μmol/L. In addition, we demonstrated that erlotinib restored intracellular accumulation of MXR in BCRP-expressing K562 cells, but did not in P-glycoprotein-expressing K562 cells. Furthermore, we showed that erlotinib selectively inhibited the P-glycoprotein-mediated efflux of VCR by a complicated mechanism, but not that of MXR. These data demonstrate for the first time that the bidirectional modulation of P-glycoprotein-mediated drug resistance by erlotinib is substrate dependent.

P-glycoprotein drug interaction sites are thought to localize to the transmembrane domains, and the presence of multiple drug binding sites has been suggested.[21] Although putative interaction sites for MXR and DOX are not well defined, the mode of interaction for DOX with P-glycoprotein seems to be different from that of *vinca* alkaloids. Specifically, substitution of P-glycoprotein

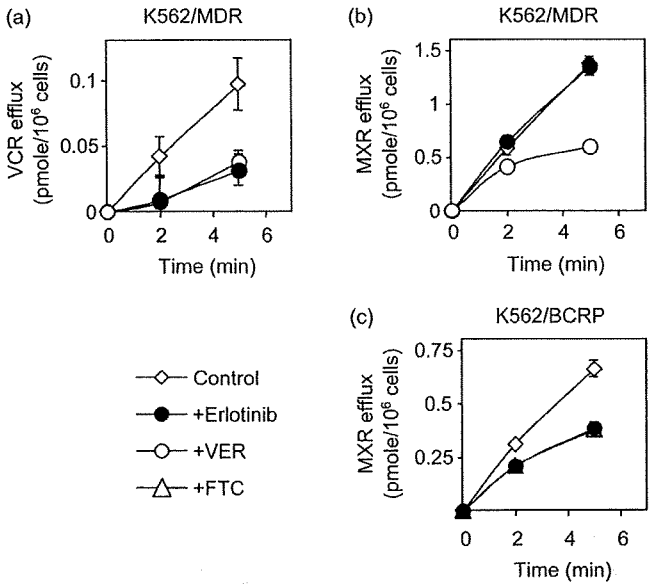

Fig. 5. Effect of erlotinib on the cellular efflux vincristine (VCR) and mitoxantrone (MXR). K562/MDR (a and b) and K562/BCRP (c) cells were pre-treated with ^{3}H-labeled substrates. Erlotinib, verapamil (VER), and fumitremorgin C (FTC) were tested to suppress efflux of incorporated substrate as described in 'Materials and Methods'. The efflux of ^{3}H-labeled substrate was determined by measuring their radioactivity levels released into the culture medium. Data are the means ± SD of triplicate determinations.

Phe-335 in transmembrane domain 6 with alanine resulted in a loss of resistance to vinblastine, but retention of resistance to DOX.[22] The RI50 value of erlotinib for DOX resistance in K562/MDR cells was approximately 10-fold higher than observed for VCR or PTX resistance (Table 2). Therefore, the region of P-glycoprotein that interacts with erlotinib may be distinct from the DOX interaction site. Further molecular studies will be required to properly elucidate the modes of interaction between kinase inhibitors and P-glycoprotein.

With regard to effects on BCRP by TKIs, previous studies have shown that gefitinib binds to ATP-bound BCRP at an as yet undetermined binding site.[23] Shi *et al.* recently reported that erlotinib did not compete with iodoarylazidoprazosin at the substrate-binding sites on BCRP or P-glycoprotein, although erlotinib stimulates the ATPase activity of both proteins.[16] Since P-glycoprotein and BCRP ATPase activities are stimulated by their substrates, and BCRP expression conferred resistance to erlotinib in PC-9 cells, erlotinib may directly interact with an as yet undetermined site in BCRP and P-glycoprotein and function like a substrate. Indeed, recent study suggests erlotinib as a substrate for both P-glycoprotein and BCRP *in vivo* since P-glycoprotein and BCRP significantly affect the oral bioavailability of erlotinib.[24]

Breast cancer resistance protein (BCRP) was more sensitive to the inhibitory effect of erlotinib than P-glycoprotein, since the RI50 values of erlotinib for BCRP were lower than those for P-glycoprotein (Tables 1 and 2). Consistently, Shi *et al.* also showed that the ATPase activity of BCRP was stimulated by lower concentrations of erlotinib than were required for P-glycoprotein.[16] In addition, gefitinib has been shown to have a higher affinity for BCRP than for P-glycoprotein.[25] Collectively, these observations

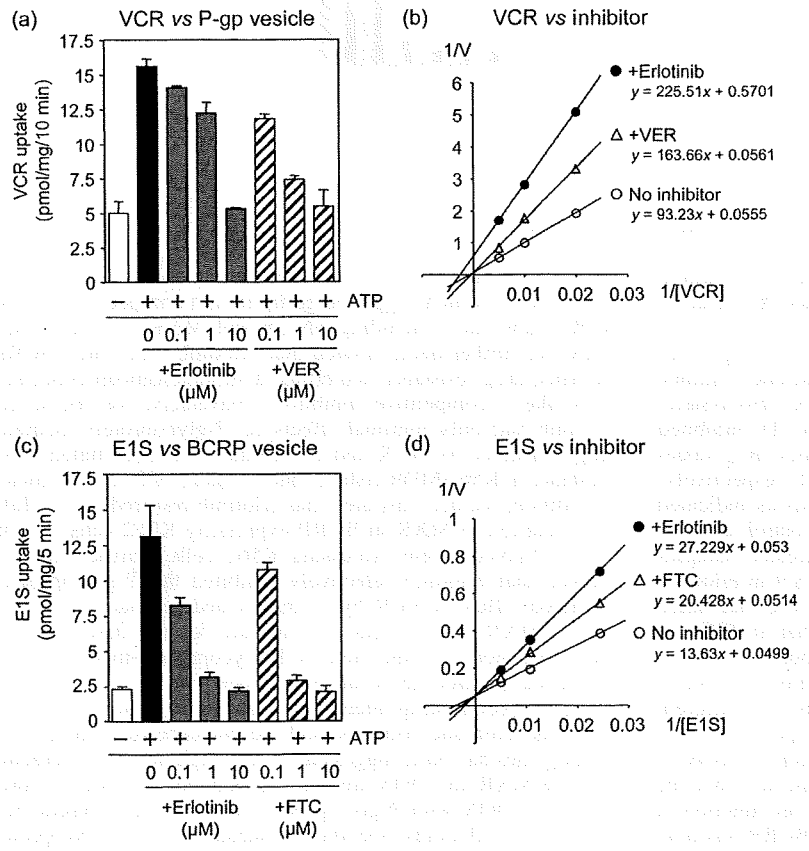

Fig. 6. The intracvesicular transports by P-glycoprotein and breast cancer resistance protein (BCRP) and Lineweaver-Burk plot analysis. Membrane vesicles from K562/MDR (a and b) and from K562/BCRP (c and d) cells were incubated for 10 min with [^{3}H]VCR (a and b) and [^{3}H]E1S (c and d) in the absence or presence of erlotinib, verapamil, or fumitremorgin C (FTC) as described in 'Materials and Methods'. The concentration of ^{3}H-labeled transporter substrate was 100 or 50 nmol/L in the experiments (a) and (c), and those in (c) and (d) were 100, 200, 400 or 50, 100, 200 nmol/L respectively. Erlotinib at 2 μmol/L and verapamil (VER) at 0.2 μmol/L were tested in experiment (c), and erlotinib at 0.13 μmol/L and FTC at 0.25 μmol/L were in experiment (d). The transport of ^{3}H-labeled substrate was determined by measuring their radioactivity levels incorporated into the membrane vesicles. Data shown in (a) and (c) are the means ± SD of triplicate determinations, and data in (b) and (d) are the means of duplicated determinations.

doi: 10.1111/j.1349-7006.2009.01213.x

suggest that erlotinib will have a higher affinity for BCRP than for P-glycoprotein.

Studies of erlotinib pharmacokinetics have shown that plasma concentrations of erlotinib are in the micromoler range in clinical situations.[26] Given that erlotinib-mediated modulation of BCRP and P-glycoprotein function was achieved at submicromoler levels in our experiments, erlotinib administration will likely affect the normal functions of BCRP and P-glycoprotein expressed in digestive organs, the kidney, and the blood–brain barrier.

Erlotinib and other TKIs will likely be tested against various tumor types in combination with chemotherapy, but the benefits of such combination therapy are not yet apparent.[27] Molecular analysis suggests that EGFR-activation mutations found in some patients are correlated with the best outcome in combination therapy with EGFR-TKIs and conventional anticancer drugs.[28] Importantly, our findings demonstrate that the pharmacological effect of erlotinib on P-glycoprotein varies among substrates. Further efforts for the understanding of pharmacological interaction between TKIs and anticancer drugs would be beneficial to improve the effectiveness of combination therapy.[29] These preclinical studies on the TKIs, the ABC transporters, and their substrates would also contribute to prevent the occurrence of unexpected adverse effects when utilizing combinational chemotherapy.

Acknowledgments

This work was supported by Grants-in-Aid from the Ministry of Education, Culture, Sports, Science and Technology; and from the Ministry of Health, Labor and Welfare, Japan. We thank Yuka Shimomura for performing the initial experiments in this work and other laboratory members for their helpful discussions.

Abbreviations

ABC	ATP-binding cassette
ATP	adenosine triphosphate
BCRP	breast cancer resistance protein
EGFR	epidermal growth factor receptor
IC_{50}	50% inhibitory concentration
TKI	tyrosine kinase inhibitor

References

1 Gottesman MM, Fojo T, Bates SE. Multidrug resistance in cancer: role of ATP-dependent transporters. *Nat Rev Cancer* 2002; **2**: 48–58.
2 Sugimoto Y, Tsukahara S, Ishikawa E, Mitsuhashi J. Breast cancer resistance protein: molecular target for anticancer drug resistance and pharmacokinetics/pharmacodynamics. *Cancer Sci* 2005; **96**: 457–65.
3 Doyle LA, Ross DD. Multidrug resistance mediated by the breast cancer resistance protein BCRP (ABCG2). *Oncogene* 2003; **22**: 7340–58.
4 Tsuruo T, Iida H, Tsukagoshi S, Sakurai Y. Overcoming of vincristine resistance in P388 leukemia in vivo and in vitro through enhanced cytotoxicity of vincristine and vinblastine by verapamil. *Cancer Res* 1981; **41**: 1967–72.
5 Fojo T, Bates S. Strategies for reversing drug resistance. *Oncogene* 2003; **22**: 7512–23.
6 Rabindran SK, Ross DD, Doyle LA, Yang W, Greenberger LM. Fumitremorgin C reverses multidrug resistance in cells transfected with the breast cancer resistance protein. *Cancer Res* 2000; **60**: 47–50.
7 Sugimoto Y, Tsukahara S, Imai Y, Ueda K, Tsuruo T. Reversal of breast cancer resistance protein-mediated drug resistance by estrogen antagonists and agonists. *Mol Cancer Ther* 2003; **2**: 105–12.
8 Katayama K, Masuyama K, Yoshioka S, Hasegawa H, Mitsuhashi J, Sugimoto Y. Flavonoids inhibit breast cancer resistance protein-mediated drug resistance: transporter specificity and structure-activity relationship. *Cancer Chemother Pharmacol* 2007; **60**: 789–97.
9 Kumar A, Petri ET, Halmos B, Boggon TJ. Structure and clinical relevance of the epidermal growth factor receptor in human cancer. *J Clin Oncol* 2008; **26**: 1742–51.
10 Harari PM, Allen GW, Bonner JA. Biology of interactions: antiepidermal growth factor receptor agents. *J Clin Oncol* 2007; **25**: 4057–65.
11 Mukai M, Che XF, Furukawa T *et al.* Reversal of the resistance to STI571 in human chronic myelogenous leukemia K562 cells. *Cancer Sci* 2003; **94**: 557–63.
12 Yanase K, Tsukahara S, Asada S, Ishikawa E, Imai Y, Sugimoto Y. Gefitinib reverses breast cancer resistance protein-mediated drug resistance. *Mol Cancer Ther* 2004; **3**: 1119–25.
13 Perez-Soler R. Erlotinib: recent clinical results and ongoing studies in non small cell lung cancer. *Clin Cancer Res* 2007; **13**: s4589–92.
14 Cohen MH, Johnson JR, Chen YF, Sridhara R, Pazdur R. FDA drug approval summary: erlotinib (Tarceva) tablets. *Oncologist* 2005; **10**: 461–6.
15 Moore MJ, Goldstein D, Hamm J *et al.* Erlotinib plus gemcitabine compared with gemcitabine alone in patients with advanced pancreatic cancer: a phase III trial of the National Cancer Institute of Canada Clinical Trials Group. *J Clin Oncol* 2007; **25**: 1960–6.
16 Shi Z, Peng XX, Kim IW *et al.* Erlotinib (Tarceva, OSI-774) antagonizes ATP-binding cassette subfamily B member 1 and ATP-binding cassette subfamily G member 2-mediated drug resistance. *Cancer Res* 2007; **67**: 11012–20.
17 Shi Z, Parmar S, Peng XX *et al.* The epidermal growth factor tyrosine kinase inhibitor AG1478 and erlotinib reverse ABCG2-mediated drug resistance. *Oncol Rep* 2009; **21**: 483–9.
18 Sugimoto Y, Sato S, Tsukahara S *et al.* Coexpression of a multidrug resistance gene (MDR1) and herpes simplex virus thymidine kinase gene in a bicistronic retroviral vector Ha-MDR-IRES-TK allows selective killing of MDR1-transduced human tumors transplanted in nude mice. *Cancer Gene Ther* 1997; **4**: 51–8.
19 Naito M, Hamada H, Tsuruo T. ATP/Mg2+-dependent binding of vincristine to the plasma membrane of multidrug-resistant K562 cells. *J Biol Chem* 1988; **263**: 11887–91.
20 Arao T, Fukumoto H, Takeda M, Tamura T, Saijo N, Nishio K. Small in-frame deletion in the epidermal growth factor receptor as a target for ZD6474. *Cancer Res* 2004; **64**: 9101–4.
21 Loo TW, Clarke DM. Mutational analysis of ABC proteins. *Arch Biochem Biophys* 2008; **476**: 51–64.
22 Loo TW, Clarke DM. Functional consequences of phenylalanine mutations in the predicted transmembrane domain of P-glycoprotein. *J Biol Chem* 1993; **268**: 19965–72.
23 Saito H, Hirano H, Nakagawa H *et al.* A new strategy of high-speed screening and quantitative structure-activity relationship analysis to evaluate human ATP-binding cassette transporter ABCG2-drug interactions. *J Pharmacol Exp Ther* 2006; **317**: 1114–24.
24 Marchetti S, de Vries NA, Buckle T *et al.* Effect of the ATP-binding cassette drug transporters ABCB1, ABCG2, and ABCC2 on erlotinib hydrochloride (Tarceva) disposition in in vitro and in vivo pharmacokinetic studies employing Bcrp1-/-/Mdr1a/1b-/- (triple-knockout) and wild-type mice. *Mol Cancer Ther* 2008; **7**: 2280–7.
25 Ozvegy-Laczka C, Hegedus T, Varady G *et al.* High-affinity interaction of tyrosine kinase inhibitors with the ABCG2 multidrug transporter. *Mol Pharmcol* 2004; **65**: 1485–95.
26 Hamilton M, Wolf JL, Rusk J *et al.* Effects of smoking on the pharmacokinetics of erlotinib. *Clin Cancer Res* 2006; **12**: 2166–71.
27 Herbst RS, Prager D, Hermann R *et al.* TRIBUTE: a phase III trial of erlotinib hydrochloride (OSI-774) combined with carboplatin and paclitaxel chemotherapy in advanced non-small-cell lung cancer. *J Clin Oncol* 2005; **23**: 5892–9.
28 Bonomi PD, Buckingham L, Coon J. Selecting patients for treatment with epidermal growth factor tyrosine kinase inhibitors. *Clin Cancer Res* 2007; **13**: s4606–12.
29 Milano G, Spano JP, Leyland-Jones B. EGFR-targeting drugs in combination with cytotoxic agents: from bench to bedside, a contrasted reality. *Br J Cancer* 2008; **99**: 1–5.

Acyl-CoA synthetase as a cancer survival factor: its inhibition enhances the efficacy of etoposide

Tetsuo Mashima,[1] Shigeo Sato,[2] Sachiko Okabe,[1] Satoshi Miyata,[3] Masaaki Matsuura,[3,4] Yoshikazu Sugimoto,[5,6] Takashi Tsuruo[7,8] and Hiroyuki Seimiya[1,9]

[1]Divisions of Molecular Biotherapy, [2]Experimental Chemotherapy, Cancer Chemotherapy Center, [3]Genome Center, [4]Division of Cancer Genomics, The Cancer Institute, Japanese Foundation for Cancer Research, Koto-ku, Tokyo; [5]Department of Chemotherapy, Faculty of Pharmacy, Keio University, Minato-ku, Tokyo; [6]Division of Gene Therapy, [7]Director's Room, Cancer Chemotherapy Center, Japanese Foundation for Cancer Research, Koto-ku, Tokyo, Japan

(Received March 26, 2009/Revised April 24, 2009/Accepted April 24, 2009/Online publication May 13, 2009)

Lipid metabolism is often elevated in cancer cells and plays an important role in their growth and malignancy. Acyl-CoA synthetase (ACS), which converts long-chain fatty acids to acyl-CoA, is overexpressed in various types of cancer. However, the role of ACS in cancer remains unknown. Here, we found that ACS enzyme activity is required for cancer cell survival. Namely, the ACS inhibitor Triacsin c induced massive apoptosis in glioma cells while this cell death was completely suppressed by overexpression of ACSL5, the Triacsin c–resistant ACS isozyme, but not by overexpression of a catalytically inactive ACSL5 mutant. ACS inhibition by Triacsin c markedly potentiated the Bax-induced intrinsic apoptotic pathway by promoting cytochrome c release and subsequent caspase activation. These effects were abrogated by ACSL5 overexpression. Correspondingly, ACS inhibition synergistically potentiated the glioma cell death induced by etoposide, a well-known activator of apoptosis. Furthermore, in a nude mouse xenograft model, Triacsin c at a non-toxic dose enhanced the antitumor efficacy of a low-dose chemotherapy with etoposide. These results indicate that ACS is an apoptosis suppressor and that ACS inhibition could be a rational strategy to amplify the antitumor effect of etoposide. (*Cancer Sci* 2009; 100: 1556–1562)

Overexpression of lipogenic enzymes is a common characteristic of many cancers.[1] In tumor cells, the supply of cellular fatty acids is highly dependent on de novo biosynthesis. FASN is a key enzyme that catalyzes the terminal step in the *de novo* synthesis of saturated fatty acids. Fatty acid synthase (FASN) is overexpressed in a wide variety of human epithelial cancer cells and plays a critical role in tumor growth and survival.[2] In addition to FASN, several other enzymes involved in lipid metabolism have recently been shown to be involved in tumor growth and malignancy.[3,4] These observations support the notion that elevated lipid metabolism could be a rational target for cancer treatment.

Acyl-CoA synthetases (ACS) are enzymes that act downstream of FASN and convert long-chain fatty acids to acyl-CoA.[5] This reaction is a crucial step in several lipid metabolism pathways, including phospholipid biosynthesis, lipid modification of cellular proteins, and β-oxidation. In mammals, five ACS isozymes have been identified. Previous reports have indicated that several ACS isozymes, such as ACSL4 and ACSL5, are overexpressed in cancer cells.[6–9] We recently identified Triacsin c, a potent inhibitor of ACS, as an agent that shows selective cytotoxicity to malignant cancer cells.[10] These observations suggest that ACS could play a predominant role in cancer cell survival. Still, however, it remains unclear how ACS regulates cell death and whether the ACS inhibition could affect the chemosensitivity of cancer.

Activation of apoptotic pathways is a key mechanism by which anticancer agents kill tumor cells.[11] Chemotherapeutic agents induce apoptosis through the intrinsic mitochondria-dependent pathway that is activated mainly by the release of cytochrome c from the mitochondria. The released cytochrome c interacts with Apaf-1 to form an Apaf-1 multimer (apoptosome), which in turn activates caspase-9 and the downstream caspases that participate in the execution phase of apoptosis.[12] The activated caspases cleave many kinds of substrates, leading to cell death. Several factors, e.g. Bcl-2 family members, suppress apoptosis on the mitochondria.[13] Because these antiapoptotic factors are frequently overexpressed in cancer cells and are involved in chemotherapy resistance, trials have been undertaken to identify their specific inhibitors, some of which are now being tested clinically.[14–16]

In the present study, we examined the antiapoptotic role of ACS in cancer cells. We found that ACS enzyme activity was essential for glioma cell survival. Moreover, we demonstrate the combinational effect of ACS inhibition with etoposide.

Materials and Methods

Chemicals. Triacsin c was purchased from Sigma (St. Louis, MO, USA). Etoposide was purchased from Bristol-Myers Squibb (New York, NY, USA). Caspase inhibitor Z-VAD-fmk and caspase substrate peptide DEVD-MCA were purchased from Peptide Institute (Osaka, Japan).

Cell culture, detection of apoptotic cells, and measurement of cell growth. Human glioma SF268 and U251 cells were cultured in RPMI-1640 supplemented with 10% heat-inactivated fetal bovine serum and 100 μg/mL kanamycin in a humidified atmosphere of 5% CO_2 and 95% air. Drug sensitivity was evaluated using the MTS method.[17] In brief, we used a CellTiter 96AQ$_{ueous}$ One Solution Cell Proliferation Assay Kit (Promega, Tokyo, Japan). Twenty microliters of MTS and phenazine ethosulfate solution were added to the drug-treated cells (100 μL/well in 96-well plates) and the mixture was incubated at 37°C for 30–60 min. For quantitation of relative cell number, OD490 was measured using a microplate reader. To detect apoptotic cells, cell nuclei were stained with Hoechst 33342.[18] Apoptotic cells were evaluated using such characteristic nuclear features as chromatin condensation and nuclear fragmentation.

Caspase and apoptosome assays. Cell lysates were prepared and caspase activity was measured using DEVD-MCA as a substrate, as described previously.[17] To estimate Bax-induced caspase activation, we transfected cells with pCGBL-HA-Bax and pGVC, a luciferase-expressing construct driven by a SV40 promoter and enhancer.[18] After transfection and subsequent drug treatment, cell lysates were prepared and caspase activity was measured. To monitor the transfection efficiency, we also measured luciferase activities in cell lysates using the Luciferase Assay System (Promega). The caspase activity was normalized by the luciferase

[8]Deceased.
[9]To whom correspondence should be addressed. E-mail: hseimiya@jfcr.or.jp

doi: 10.1111/j.1349-7006.2009.01203.x

activity to estimate relative Bax-dependent caspase activation. To measure apoptosome activity, cytosolic extracts were prepared as described previously[17] and incubated with 10 μM cytochrome c and 1 mM dATP for 20–40 min. After the incubation, caspase activity was measured.

Subcellular fractionation and western blot analysis. Subcellular fractions were obtained by using a ProteoExtract Subcellular Proteome Extraction kit (Calbiochem, San Diego, CA, USA). Each extract derived from the same number of the cells was subjected to SDS-PAGE. To analyze apoptosis regulators' expression, we washed cells in ice-cold phosphate-buffered saline (PBS) and lyzed them in TNE buffer (10 mM Tris-HCl [pH 7.8], 1% Nonidet P-40, 150 mM NaCl, 1 mM EDTA, and 10 μg/mL aprotinin) on ice for 30 min. After centrifugation at 12 000*g* for 10 min at 4°C, the supernatant (TNE lysate) was subjected to SDS-PAGE. For detection of cytochrome c release from the mitochondria, cytosolic extracts were prepared as described previously[10] and were subjected to SDS-PAGE. Western blot analysis was performed as described previously[19] with the following primary antibodies: mouse anti-FLAG (M2; Sigma), mouse anti-PARP (BD Pharmingen, San Diego, CA, USA), rabbit anti-EGFR (Cell Signaling Technology, Beverly, MA, USA), mouse anti-voltage-dependent anion channel (VDAC) (Ab-4; Calbiochem), mouse anti-cytochrome c (7H8.2C12; BD Pharmingen), rabbit anti-HA (Y-11; Santa Cruz Biotechnology, Santa Cruz, CA, USA) mouse anti-α-tubulin (B5-1-2; Sigma), mouse anti-Bcl-2 (BD Pharmingen), mouse anti-Bcl-XL (BD Pharmingen), or mouse anti-Bax (BD Pharmingen).

Immunofluorescence staining. Cells were fixed with 2% paraformaldehyde/PBS and permeabilized with 0.5% NP40/PBS. The fixed cells were blocked in PBS containing 1% bovine serum albumin and incubated with rabbit anti-FLAG (Sigma) and mouse anti-cytochrome c (6H2.B4; BD Pharmingen) antibodies. These primary antibodies were detected with Rhodamine-conjugated anti-rabbit Ig and FITC-conjugated anti-mouse Ig, respectively. DNA was stained with 0.2 μg/mL of DAPI. Images were acquired using an Olympus IX-71 microscope with a DP70 digital camera and Lumina Vision software (Mitani Corporation, Tokyo, Japan).

Vector construction. For the expression of human ACSL5 and its inactive mutant ACSL5-MT, pHa-ACSL5-FLAG-IRES-DHFR and pHa-ACSL5-MT-FLAG-IRES-DHFR were constructed as described previously.[10,20] To construct an ACSL5 mutant, delta L, that lacked an amino-terminus sequence (amino acid 2–41), we amplified, by polymerase chain reaction (PCR), the ACSL5 fragment that lacked amino acids 2–41 and subcloned it into the pHa vector to generate pHa-ACSL5 (delta L)-FLAG-IRES-DHFR. The full-length cDNA for human Bax was amplified by PCR and subcloned into a pCGBL mammalian expression vector with an N-terminal HA epitope tag to generate pCGBL-HA-Bax.

Transient transfection and retroviral infection. Transient transfection of pCGBL-HA-Bax was performed using Lipofectamine 2000 (Invitrogen, San Diego, CA, USA). For retroviral gene transfer, PA317 cells were transfected with pHa-IRES-DHFR (mock), pHa-ACSL5-FLAG-IRES-DHFR, or ACSL5 mutant constructs, selected with methotrexate (MTX), and culture supernatants of the MTX-resistant PA317 cells were added to SF268 cells, as described previously.[10] After retroviral infection and subsequent methotrexate selection (100 ng/mL), stably transduced cells were established.

Acyl-CoA synthetase (ACS) enzyme assay. Total cell lysates were prepared by homogenizing cells in buffer A, and the ACS activity was measured, as described previously.[10] In brief, the assay mixture contained 1.2 μM $MgCl_2$, 5 μM ATP, 3 μM potassium fluoride, 0.1 μM coenzyme A, 3 μM 2-mercaptoethanol, and 0.03 μM palmitic acid with 0.1 μCi of [^{14}C]-palmitic acid in a total volume of 20 μL. The reaction was initiated by adding 10 μL of cell lysates at 37°C and terminated after 1 h by adding 270 μL of isopropanol-heptane-aqueous 1 M H_2SO_4 (40:10:1 by volume). Then 180 μL of heptane and 120 μL of water were added and the upper layer was discarded. The lower layer was washed twice with 200 μL of heptane containing 15 mM palmitic acid and the radioactivity in 100 μL of the sample was counted in 1 mL of ACS II (Amersham, Tokyo, Japan).

Mouse xenograft therapeutic model. U251 cells (5×10^6 cells/mouse) were implanted subcutaneously in the right flanks of 6-week-old CAnN.Cg-Foxn1nμ/CrlCrlj nude mice (Charles River Laboratories Japan, Kanagawa, Japan). Therapeutic experiments (five mice per group) were started approximately 20 days after implant when tumors reached 90–170 mm^3, as measured with calipers (day 0). Etoposide (12 mg/kg/day) was administered i.v. on days 0, 1, and 2. Triacsin c (4 mg/kg/day) was administered by intratumoral injection in 40 μL of saline on days 0, 1, and 2. Control mice received the same volume of saline as the experimental mice. The length (L) and width (W) of the tumor mass were measured, and the tumor volume (TV) was calculated as: $TV = (L \times W^2)/2$. The difference in the growth rate between etoposide-treated and the etoposide + Triacsin c–treated groups was tested by an autoregressive random errors model[21] using statistical software R[22] (version 2.7.1) with the agce package (version 1.2; http://www.R-project.org). All animal procedures were performed in the animal experiment room of the Japanese Foundation for Cancer Research (JFCR) using protocols approved by the JFCR Animal Care and Use Committee.

Results

Acyl-CoA synthetase (ACS) activity contributes to cancer cell survival. We have shown that Triacsin c, a specific inhibitor of ACS, induces cell death preferentially in tumor cells, but is less toxic to non-cancerous cells.[10] To confirm the requirement for ACS enzyme activity in cancer cell survival, we established cell lines that stably overexpressed either ACSL5 or its inactive mutant (ACSL5-MT), since ACSL5 is a Triacsin c–resistant isozyme among five ACS members,[23] and we postulated that the overexpression of ACSL5 could effectively reverse the inhibition of ACS activity by Triacsin c. We chose glioma cell lines for this experiment since ACSL5 is frequently overexpressed in malignant glioma.[7] When retrovirally transduced in human glioma SF268 cells, wild-type ACSL5 and the ACSL5-MT proteins were stably expressed (Fig. 1a, inset). On the other hand, the ACS activity was exclusively increased in the wild-type ACSL5-expressed cells but not in ACSL5-MT-expressed cells under both Triacsin c–treated and –untreated conditions (Fig. 1a). Triacsin c inhibition of ACS activity was eliminated by wild-type ACSL5 but not by ACSL5-MT. These data indicate that ACSL5-MT acts as an inactive mutant and that these systems work to determine the role of ACS activity in cancer cell survival. We examined the effect of wild-type ACSL5 and ACSL5-MT on Triacsin c–induced SF268 cell death. As shown in Fig. 1(b,c), Triacsin c (3 μM) strongly induced apoptosis and activated caspases in mock cells. Wild-type ACSL5, which retained ACS activity in Triacsin c–treated cells, completely inhibited the caspase activation and apoptotic cell death, while ACSL5-MT did not (Fig. 1b–d). Triacsin c–induced cell death would depend on caspase activation because a caspase inhibitor, Z-VAD-fmk, restored the viable cell number (Fig. 1d). These results indicate that ACS plays an essential role in SF268 cell survival, and that ACS inhibition induces apoptosis of the cells.

Role of subcellular ACS in cancer cell survival. As shown above, ACSL5 overexpression compensated for the decrease of ACS activity in Triacsin c–treated cells and suppressed Triacsin c–induced cell death. Since rat ACSL5 is expressed predominantly on the mitochondrial membrane,[24] we speculated that human ACSL5 could also be expressed on the organelle and would compensate for Triacsin c–induced loss of the ACS activity, leading to cell death suppression. To test this hypothesis, we first examined the subcellular localization of human ACSL5 by immunofluorescence staining (Fig. 2a). Consistent with the

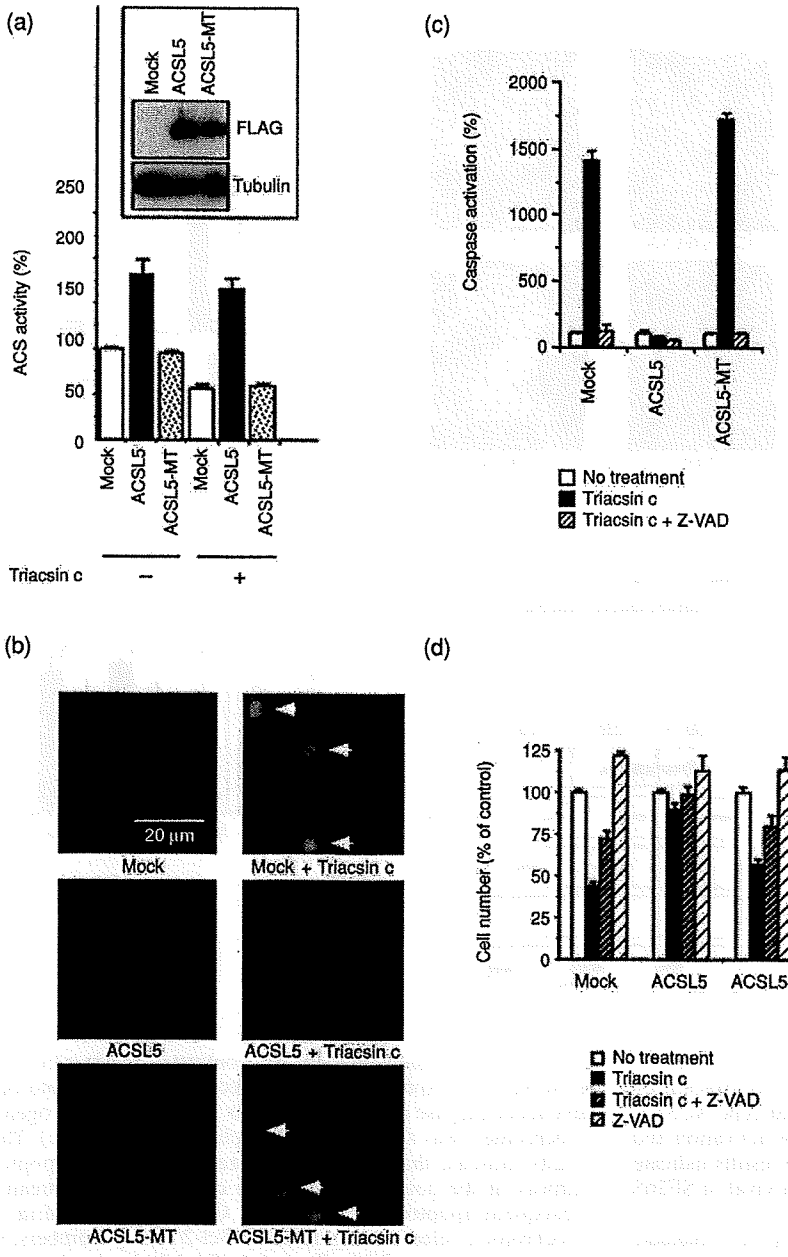

Fig. 1. Acyl-CoA synthetase (ACS) catalytic activity requirement for glioma cell survival. (a) Effect of 48-h Triacsin c treatment (3 μM) on ACS activity in mock-, ACSL5-, and ACSL5-MT–transduced SF268 cells. ACS activity was measured as described in 'Materials and Methods'. Inset, The expressions of ACSL5 and ACSL5-MT were examined by western blot with anti-FLAG M2 antibody. The expression of α-tubulin was analyzed as a loading control. (b) Apoptosis induction after Triacsin c treatment. Cells were treated as in (a). The cell nuclei were stained with Hoechst 33342. Induction of apoptosis in each cell was evaluated using the characteristic nuclear features of apoptosis, such as chromatin condensation and nuclear fragmentation. Arrows indicate apoptotic cells. (c) Caspase activation after Triacsin c treatment. Cells were left untreated or treated with 3-μM Triacsin c in the absence or the presence of 50-μM caspase inhibitor, Z-Val-Ala-Asp(OMe)-CH2F (Z-VAD), for 30 h. Caspase activity was measured as described in 'Materials and Methods'. (d) Cell number after Triacsin c treatment. Cells were treated as in (c) for 48 h and relative cell number was measured using the 3-(4,5-dimethylthiazol-2-yl)-5-(3-carboxymethoxyphenyl)-2-(4-sulfophenyl)-2H-tetrazolium (MTS) method, as described in 'Materials and Methods'. Data are mean values of three independent experiments. Error bars show standard deviations.

previous report of rat ACSL5, human ACSL5 was colocalized with cytochrome c, a marker protein of mitochondria. Furthermore, the patterns of immunofluorescence staining suggested that the human ACSL5 was localized not only to the mitochondria but could also exist at the perinuclear region and, to a lesser extent, in the nucleoplasm (Fig. 2a). To determine the localization of human ACSL5 further, we performed subcellular fractionation of cellular proteins. As shown in Fig. 2(b), ACSL5 was not only present in the organelle/membrane fraction (O/M), which contained mitochondria, but also in the nuclear fraction (N). These data confirmed that ACSL5 was localized in the nuclei of cancer cells as well as to the mitochondria. To clarify the importance of subcellular ACS in SF268 cell survival, we generated deletion mutants of ACSL5 and examined their subcellular localizations. We found that the mutant delta L (Fig. 2b) exclusively lost its nuclear localization, although the amino-terminus sequence that the mutant lacked did not contain any nuclear localization sequence (data not shown, searched by the PSORT II prediction algorithm at http://psort.ims.u-tokyo.ac.jp/form2.html). On the other hand, this mutant still retained the organelle localization and ACS activity. When retrovirally transduced in SF268 cells, both wild-type ACSL5 and the delta L proteins were stably expressed, and, as in the wild-type ACSL5-expressed cells, ACS activity clearly increased in the delta L–expressed cells (Suppl. Fig. 1). These results indicated that the delta L was catalytically active. While the wild-type ACSL5 was detected in both the organelle/membrane and the nuclear fractions, the delta L mutant lost its nuclear localization and instead was included in the organelle/membrane and the cytosol (C) fractions (Fig. 2b). Immunofluorescence staining further revealed that the delta L was still localized to the mitochondria (Suppl. Fig. 2). These data indicate that the N-terminal region deleted in the delta L mutant is required for

doi: 10.1111/j.1349-7006.2009.01203.x

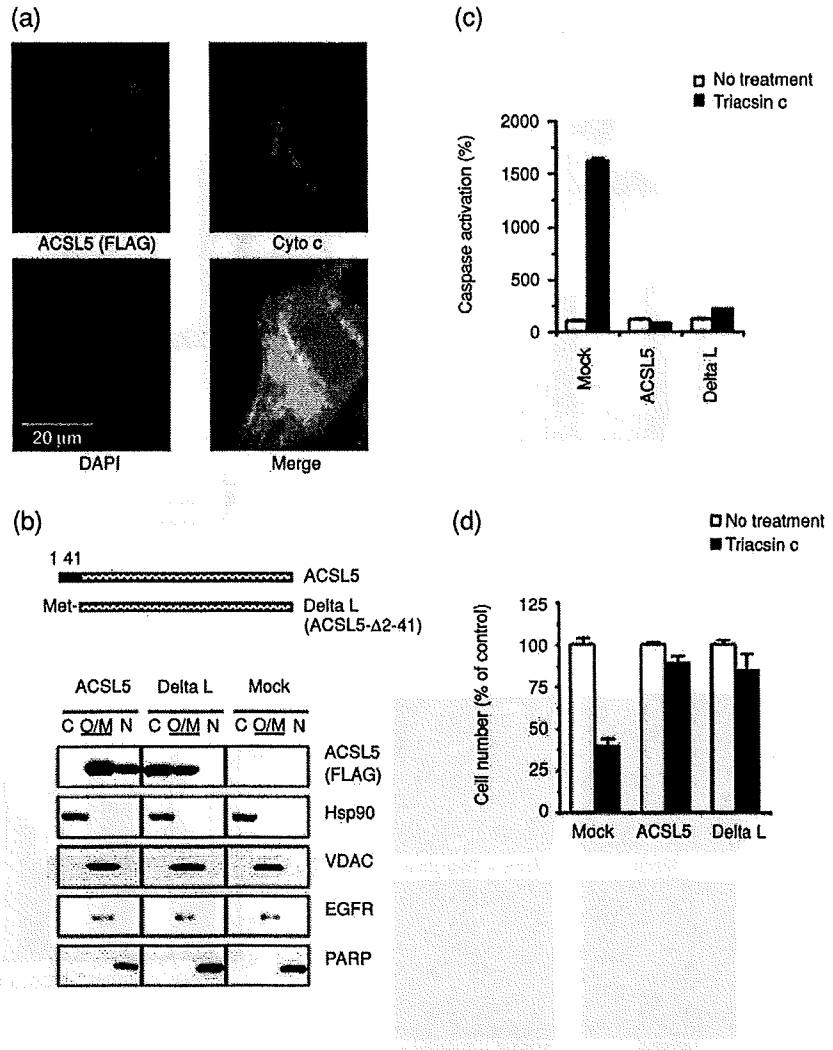

Fig. 2. Organelle-localized acyl-CoA synthetase (ACS) is critical for cancer cell survival. (a) Localization of human ACSL5 in SF268 cells. ACSL5 (FLAG) and the mitochondria marker cytochrome c (Cyto c) were detected by indirect immunofluorescence stain of ACSL5-transduced SF268 cells with anti-FLAG M2 (red) and anti-cytochrome c (green) antibodies, respectively. DAPI staining of DNA is shown in blue. (b) Subcellular fractionation of ACSL5 and its N-terminal deletion mutant (delta L) in SF268 cells. Cytoplasmic (C), organelle/membrane (O/M), and nuclear (N) fractions were prepared, and subjected to western blot analysis with the indicated primary antibodies. Blots with anti-FLAG M2 antibody (FLAG) indicate the expression of ACLS5. Blots with anti-Heat shock protein (Hsp)-90, voltage-dependent anion channel (VDAC), epidermal growth factor receptor (EGFR), and poly(ADP-ribose) polymerase (PARP) antibodies demonstrate the purity of their respective fractions. (c) Caspase activation in SF268/ACSL5 and SF268/delta L cells after Triacsin c treatment. Mock-, ACSL5-, and delta L–transduced SF268 cells were left untreated or treated with 3-μM Triacsin c for 30 h. Caspase activity was measured as described in 'Materials and Methods'. (d) Cell number after Triacsin c treatment. Cells were treated as in (c) for 48 h and relative cell number was measured using the 3-(4,5-dimethylthiazol-2-yl)-5-(3-carboxymethoxyphenyl)-2-(4-sulfophenyl)-2H-tetrazolium (MTS) method. In (c) and (d), data are mean values of three independent experiments, and error bars show standard deviations.

ACSL5 targeting to the nuclei but not to the mitochondria. We compared the effect of ACSL5 and the delta L on Triacsin c–induced cell death and found that, as well as wild-type ACSL5, the delta L mutant efficiently suppressed caspase activation and cell death caused by Triacsin c (Fig. 2c,d). These results indicate that the nuclear ACS could not be required for survival of SF268 cells.

Enhancement of the intrinsic apoptosis pathway by ACS inhibition. To determine the role of ACS in glioma cell survival, we examined whether ACS could act as a repressor against mitochondria-dependent apoptosis. Mitochondrial apoptosis inducers, such as Bax protein, can directly activate this intrinsic apoptosis pathway.[25,26] Therefore, we tested the effect of ACS inhibition on Bax-induced apoptosis. As shown in Figure 3(a), Bax activated caspases in a dose-dependent manner. Sublethal dose of Triacsin c potentiated this Bax-induced caspase activation. Moreover, this effect was strongly suppressed by compensation of ACS activity by ACSL5 overexpression. These results indicate the antagonistic role of ACS in the mitochondrial apoptosis pathway, and ACS inhibition potentiates this pathway. To clarify the molecular mechanisms further, we examined the effect of ACS inhibition on Bax-induced cytochrome c release from the mitochondria to cytoplasm. When cells were expressed with Bax alone, cytochrome c release to the cytosol was below detection levels in western blot analysis. On the other hand, we found that the cytochrome c release was clearly enhanced by Triacsin c, which was suppressed by ACSL5 expression (Fig. 3b). By contrast, Triacsin c treatment or ACSL5 overexpression did not affect the *in vitro* apoptosome-dependent caspase activation that was initiated when exogenous cytochrome c was added to the cytosolic extracts (Fig. 3c). These results indicate that ACS antagonizes the intrinsic apoptosis pathway at the point of cytochrome c release and upstream of subsequent apoptosome activation. On the mitochondria, the cytochrome c release is regulated by Bcl-2 family members.[13,15] So next, we examined the effect of ACS inhibition on the protein expression of the apoptosis regulators in mock and ACSL5-overexpressed cells. We found that ACS inhibition did not affect protein levels of the mitochondrial Bcl-2 family members, Bcl-2, Bcl-XL, and Bax (Suppl. Fig. 3), suggesting the involvement of other factors in the apoptosis enhancement.

Potentiation of etoposide-induced cell death by ACS inhibition. Because ACS inhibition potentiated activation of the intrinsic apoptosis pathway, we examined whether ACS inhibition also enhances chemotherapeutic agent–induced death of cancer cells. We initially examined combinations of several chemotherapeutic drugs with Triacsin c, and determined the optical conditions for maximal efficacy. As a result, we found the synergistic effect of ACS inhibition with etoposide. As a result, we found the combinational effect of Triacsin c with etoposide, which induces apoptosis through the mitochondria-mediated pathway.[27,28] When SF268/mock cells were treated with either etoposide (0.3 μg/mL, 48 h) or a sublethal dose of Triacsin c (1 μM, 48 h), caspases were